# Surface Modification of pHEMA with Phenylboronic-Acid for Corneal Regeneration

# Surface Modification of pHEMA with Phenylboronic-Acid for Corneal Regeneration

By

NADEEN SHAABANA, B.SC HONOURS BEHAVIOUR, COGNITION AND NEUROSCIENCE

A Thesis

Submitted to the School of Graduate Studies

In the Partial Fulfillment of the Requirements

For the Degree

Master of Applied Science

McMaster University

MASTER OF APPLIED SCIENCE (2018) McMaster University

(Biomedical Engineering) Hamilton, Ontario

TITLE: Surface Modification of pHEMA with Phenylboronic-Acid for Corneal Regeneration

AUTHOR: Nadeen Shaabana, BSc. Honours Behaviour, Cognition and Neuroscience

(University of Windsor)

SUPERVISOR: Professor Heather Sheardown

NUMBER OF PAGES: vii, 54

**Abstract**

Corneal diseases and insults can result in opacification of the cornea and ultimately lead to blindness. Treatment options for patients are limited due to limited donor availability and the fact that many patients are not eligible for certain treatments due to the nature of their condition. When conventional treatment options are not beneficial for a patient, artificial corneal replacement is necessary. Current artificial replacements induce epithelial downgrowth, where the remaining host corneal cells grow underneath the replacement ultimately leading to implant extrusion. Therefore, surface modification of these synthetic materials is necessary in order to allow proper epithelialization on the surface.

This work focuses on the creation of a novel corneal scaffold consisting of poly(2-hydroxyethyl methacrylate) (pHEMA) which is surface modified by 3-(acrylamido)phenylboronic acid (APBA), a molecule known to have cell-binding properties through its ability to bind sugars found throughout the cell membrane. Surfaces were modified using two different polymerization techniques: conventional free radical polymerization (CFRP) and a controlled polymerization technique known as atom transfer radical polymerization (ATRP). It was hypothesized that ATRP would yield more uniform APBA brushes than the conventional method, and therefore create a more efficient cell-binding surface than the conventional method.

Following each modification, the surface chemical composition of the materials was confirmed by ATR-FTIR, XPS and surface wettability measurements. Once prepared, NIH 3T3 mouse embryo fibroblasts were seeded onto the surfaces and cell viability was assessed through an MTT assay. The results revealed no cell viability on the APBA-modified surfaces, with surface hydrophobicity, grafting density and surface toxicity (for surfaces modified through ATRP) contributing to the lack of cell attachment.

**Acknowledgements**

There are many people whom I would like to thank for their support during my time here. First and foremost, I would like to thank my supervisor, Dr. Heather Sheardown. You always make time for your students and always relieved any stresses or anxieties I had about my work. I've learned so many things during my time with you and I appreciate all of your support every step of the way.

I would also like to thank my lab mates for all of their help and expertise. I would like to thank Lina who really is the "knower of all things". You showed me how to do just about everything, and always found the time to help even though you're busy doing everything else. Thank you for keeping me from feeling completely lost, none of us would know what to do without you. Jennifer, thank you for your help with making materials through ATRP, I wish you all the luck with school. I would also like to thank everyone else in the Sheardown lab (Fran, Talena, Fei, Jeff, Alysha, Ben, Ivana, Aakash, Vida, Musa, Emily-Anne, Mitch, Eva, Samuel and Erin), we all know very different things so we can always count on each other for help, no matter the problem.

Next, I would like to thank all the friends I have made throughout these two years. To Jess, thank you for being my 4-months-late twin. I enjoyed being blissfully unaware of all the responsibilities we had during our first year, playing squash and going to Banff, and then entering complete misery and stress when we realized just how much we have to do. It's been stressful, but it's also been the best time. To Sharita, thank you for taking me out every time I felt stressed out, which was basically every night. I will never forget our late-night drives and impromptu hikes and Toronto trips. This master's would not have been the same without you. To Rana and Celine, thank you for providing me with endless entertainment (even when I should have been working) and always being there for me if I needed advice, you guys are the best.

Julia, I've never met someone that has impacted my life so much in such a short period of time. From passing out in my car from eating pizza and crêpes, to seeing 3 concerts in the span of 4 days. We've had some greats chats, some great laughs and I'm looking forward to so much more. Marisa, you're the kindest and sweetest person I've ever met. You've taught me so much in the little time that I've known you and I believe that you have such a bright future ahead of you. Finally, to my long-time friend and roommate Sarah. Thank you for all the laughs and the paper-editing, it was always nice to unwind after a long day and stay up late watching DIY videos, vine compilations, and all of the old Disney movies.

At last, I would like to thank my family. My parents have always supported me and been there for me, regardless of what I chose to do. Thank you for all that you do for me, I am forever grateful. I especially would like to thank my brother, Ala. Thank you for literally walking me through everything. You were there for me when I was home-sick, you were there for me when I was stressed and always had patience when I was being stubborn. These two years would have been impossible without you by my side. Thank you for being there for me, in more ways than you think.

## Table of Contents

## List of Figures

## List of Tables

## List of Schemes

## List of Abbreviations

| | |
|---|---|
| ACN | Acetonitrile |
| AIBN | 2,2'-Azobis(2-methylproprionitrile |
| APBA | 3-(Acrylamido)phenylboronic acid |
| ATR-FTIR | Attenuated total reflectance-fourier transform infrared spectroscopy |
| ATRP | Atom transfer radical polymerization |
| BBIB | Benzyl bromo isobutyrate |
| BPY | 2,2-Bipyridyl |
| CFRP | Conventional free radical polymerization |
| CLRP | Controlled living radical polymerization |
| COMET | Cultivated oral mucosal epithelial transplantation |
| DCM | Dichloromethane |
| DMEM | Dulbecco's Modified Eagle Medium |
| DMF | N,N-dimethylformamide |
| DMSO | Dimethyl sulfoxide |
| ECM | Extracellular matrix |
| EDTA | Ethylenediaminetetraacetic acid |
| EGDMA | Ethylene glycol dimethacrylate |
| EtOH | Ethanol |
| FBS | Fetal bovine serum |
| $H_2O$ | Water |
| HEMA | 2-hydroxyethyl methacrylate |

| | |
|---|---|
| IPN | Interpenetrating network |
| KPro | Keratoprosthesis |
| LESC | Limbal epithelial stem cells |
| LSCD | Limbal stem cell deficiency |
| MACL | Methacryloyl chloride |
| MeOH | Methanol |
| MMEQ | Monomethyl ether hydroquinone |
| MTT | 3-(4,5-dimethylthiazol-2-yl)-2,5-diphenyltetrazolium bromide |
| NaCl | Sodium chloride |
| PBA | Phenylboronic acid |
| PDMS | Polydimethylsiloxane |
| PMMA | Poly(methyl methacrylate) |
| polyHEMA/pHEMA | Poly(2-hydroxyethyl methacrylate) |
| SA | Sialic acid |
| TEA | Triethylamine |
| XPS | X-ray photoelectron spectroscopy |

# 1. Introduction

## *1.1. Corneal Diseases and Treatment Options*

Corneal diseases are a major contributor to vision loss and blindness, secondary only to cataracts. Worldwide, 120 million people suffer from vision problems due to corneal opacification as a result of injury or disease, and 10 million of those people suffer from complete corneal blindness[7]. Opacification can either be the result of thermo- or chemical burns, or as a result of immunological disorders and ocular diseases (e.g., Stevens-Johnson Syndrome). These cases often result in a deficiency in limbal stem cells, which are the cells responsible for corneal regeneration and wound healing[8]. However, limbal stem cell deficiency (LSCD) can also be acquired through genetic diseases, surgeries, neurotrophic keratitis, and topical medications. The epithelium is the smooth, transparent, outermost layer of the cornea that protects the cornea from the external environment, whereas the conjunctiva is a thick layer of cells that protects the rest of the eye. The corneal limbus acts as the barrier between these two regions. The aforementioned diseases and disorders can often cause damage to the limbus or a deficiency in its constituent cells, and ultimately disrupt its barrier function. Once destroyed, conjunctivilization may occur in which the conjunctiva begins to grow over the cornea and cause opacification. Furthermore, destruction of the limbus effectively destroys the microenvironment for limbal epithelial stem cells, which ultimately leads to a deficiency in these cells[9].

The standard treatment for corneal degeneration is donor graft transplantation. Although this method has been successful and in use for approximately 30 years, it remains problematic for several reasons. Aside from limited donor availability, patients that suffer from burns, severe dry eye, immunological disorders, vascularization or ocular diseases are not suitable candidates for these transplantations due to chronic inflammation.

One alternative to donor graft transplantations is stem cell transplantation to regenerate the damaged corneal epithelium. Unilateral cases allow for the autologous transplantation of limbus from the healthy eye into the affected eye, eliminating the need for immunosuppressive drugs. However, this method can increase the incidence of LSCD in the healthy eye. Bilateral cases usually require a limbal donor. Another option for these patients is the transplantation of oral mucosal epithelial cells. This method also bypasses the need for immunosuppressive drugs as they can come from the patient's own mouth. However, this epithelium does not remain completely transparent and eventually begins to cloud the cornea once more[9].

Extensive research has explored artificial corneal replacements, or keratoprostheses (KPro), for patients are not suitable candidates for the aforementioned treatment options due to either the nature of the pathology or severity of corneal damage. These artificial replacements are constructed from either biological (e.g., collagen) or synthetic (e.g., polymer) materials, with properties that are favourable for cell adhesion and proliferation, while also being biocompatible and maintaining transparency[8,10,11]. In order to generate these properties, the surface chemistry or topography of these materials is often modified in order to optimize cellular interactions and biocolonization of the material by remaining host corneal cells[12].

Over the years, several materials have been used to construct synthetic KPros, including polymers such as poly(2-hydroxyethyl methacrylate) (pHEMA), poly(methyl methacrylate) (PMMA), and polydimethylsiloxane (PDMS)[13–16]. Each polymer was chosen for certain desirable properties, such as the high oxygen permeability of PDMS and the low toxicity of pHEMA. However, without any modification, none of these materials are suitable candidates for corneal replacements, as they are unable to promote epithelialization onto their surfaces.

In order to better promote cell growth and adhesion to these surfaces, surface chemistry is modified in order to allow for the tethering of other entities such as cell adhesion molecules and cell mitogens. One such mitogen that has gained considerable attention in bioengineering is boronic acid. Boronic acids or macromolecules that contain boronic acids have been implicated in a wide variety of biomedical applications. They have been used to functionalize hydrogels, nanoparticles and sensors for the detection and treatment of type-1 diabetes. Furthermore, they have been shown to play a critical role in cell adhesion and cell culture [17,18].

Boronic acids are capable of reversibly binding to glycoproteins found at cell surfaces. In cell culture, trypsin is often used to detach cells from the surface. Trypsin can digest cell attachment proteins and can lead to overall damage to the cell. However, boronic acids may provide a route for cell detachment without the use of trypsin. Cells can be readily detached from surfaces through the addition of D-sorbitol or D-fructose solutions due to the competitive binding of the sugars that occurs with the boronic acid residues on the polymer surface. Boronic acids are able to promote cell attachment through their interaction with glycoproteins that are responsible for mediating cell adhesion, such as fibronectin or laminin. [17–19].

The technique used for grafting polymer brushes onto a surface can greatly influence the efficiency of these surfaces as biomaterials[20]. Generally, there are two approaches for polymer attachment onto a surface: “grafting to” and “grafting from”. While the former is not difficult to synthesize, the latter is capable of creating polymer brushes with greater control and precision. This implies that the material’s surface is first chemically modified with an initiator monolayer, which then serve as direct sites for polymer chain growth. Conventional free-radical polymerization (CFRP) and atom transfer radical polymerization (ATRP) are two polymerization techniques that can be employed through this approach. ATRP has gained considerable attention

due to its robust nature and capability to control surface density and chain length[21], unlike CFRP. Although both of these polymerization techniques will result in surfaces with boronic acid polymer chains, ATRP may create surfaces with more uniform polymer chains and may lead to more favourable cell adhesion and proliferation for corneal restoration. To our knowledge, there has been minimal work investigating the modification of a corneal scaffold with phenylboronic acid using CFRP and ATRP. The hypotheses made in this work are that surfaces modified with phenylboronic acid will have greater cell viability than surfaces that are unmodified. Furthermore, surfaces that are modified using ATRP will have greater cell viability than surfaces modified through CFRP, due to the controllability of the latter technique which will yield a surface with a more uniform polymer brush layer.

### *1.2. Overall Objectives*

The overall objective of this research is to construct a surface-modified polymer that has potential to serve as a scaffold that promotes corneal epithelial and potentially corneal limbal stem cell adhesion and proliferation. The polymer should be modified in a manner that renders its surface favourable for attachment of mitogens.

When grafted on the surface, phenylboronic acid should be oriented such that it allows for the interaction with cell surface carbohydrates. These modifications should be characterizable and quantifiable in terms of chemical composition and change in surface wettability. Cell seeding should demonstrate a greater cell viability in comparison to the unmodified surface, with proper cell morphology, density and spread.

### *1.3. Thesis Outline*

This thesis is organized into five chapters. The first chapter serves as an introduction to the topic of this research and presents the overall objectives of the project and the thesis outline.

The second chapter includes the literature review, which will discuss the fundamental topics relating to this research such as the mechanism for the natural shedding process of the epithelium layer and corneal wound healing following minor injuries. Additionally, the review will discuss current treatments for more severe corneal injury, including artificial corneal replacements and the materials and surface modification techniques used for these replacements. The third and fourth chapter will contain the materials and methods and the results and discussion, respectively. The fifth chapter discusses concluding and further remarks, followed by all literature references and the appendix.

## 2. Literature Review

### *2.1. The Cornea*

The cornea is the transparent window of the eye and is one of the structures that makes up the anterior segment of the eye, along with the lens, sclera, conjunctiva and the tear film (Figure 1). As the outermost layer of the eye, it is avascular and functions as the structural and infectious barrier. Along with the lens, it is the light refracting surface of the eye, providing approximately two-thirds of the optical power [1,22]. The bulbar or ocular conjunctiva covers the sclera and consists of approximately six to nine layers of epithelial cells[23]. The limbus is the border separating the cornea from the sclera. It acts as a barrier that prevents the conjunctiva from entering into the cornea (conjunctivilization), a pathway for aqueous humour discharge; as well as a source of epithelial stem cells important in the regulation of corneal health [24]. The tear film covers the cornea, it is a thin layer that provides with nutrients and maintains the cornea's optical qualities[25].

As illustrated in Figure 1, the cornea consists of three cellular layers and two interface layers. From anterior to posterior, the three cellular layers are the corneal epithelium, stroma and endothelium; and the two interface layers are Bowman's layer and the Descemet's membrane.

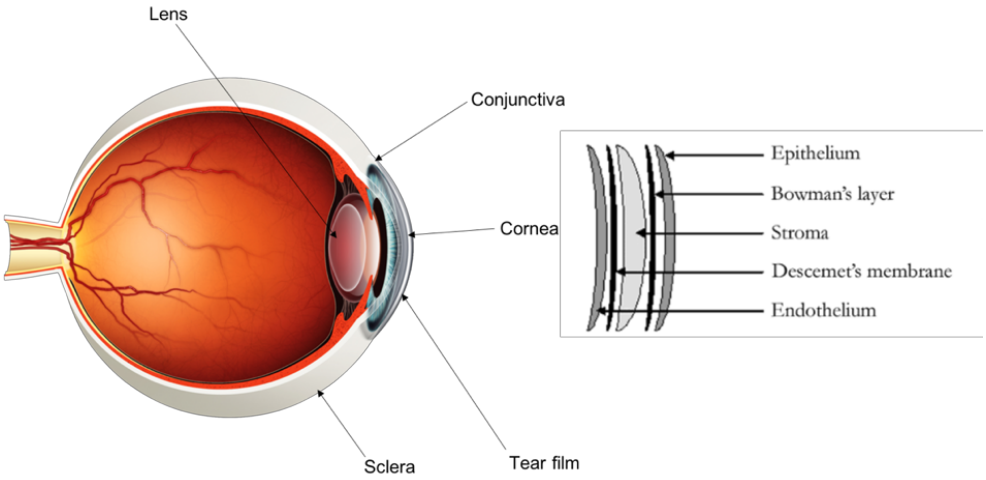


**Figure 1.** Illustration depicting the cross section of the eye, depicting the structures that encompass the exterior eye as well as the five layers of the cornea. Images adapted from: https://www.lei.org.au/services/eye-health-information/eye-diagram/ and https://www.cornealdystrophyfoundation.org/what-is-corneal-dystrophy

### *2.1.1. Epithelium*

The epithelial layer is the outermost layer, providing a barrier between the internal ocular structures and the external surrounding environment. This layer is approximately 40-50μm thick, with 4-6 layers of non-keratinized squamous cell (Figure 2)[1,26] and is critical to the refraction of light by the cornea. The anterior portion of the epithelial layer is covered by the tear film, which serves as a refractive surface for the eye, evening out the microirregularities present on the surface of the cornea. Conjunctival goblet cells produce the tear film's mucinous layer, which in turn interacts with the corneal epithelial cell glycocalyx, creating a hydrophilic interface between the cells and the aqueous portion of the tears. In addition to its contribution to the cornea's optical function, the tear-film also protects the corneal surface from physical and microbial damage and provides immunological and growth factors that help maintain epithelial health[27].

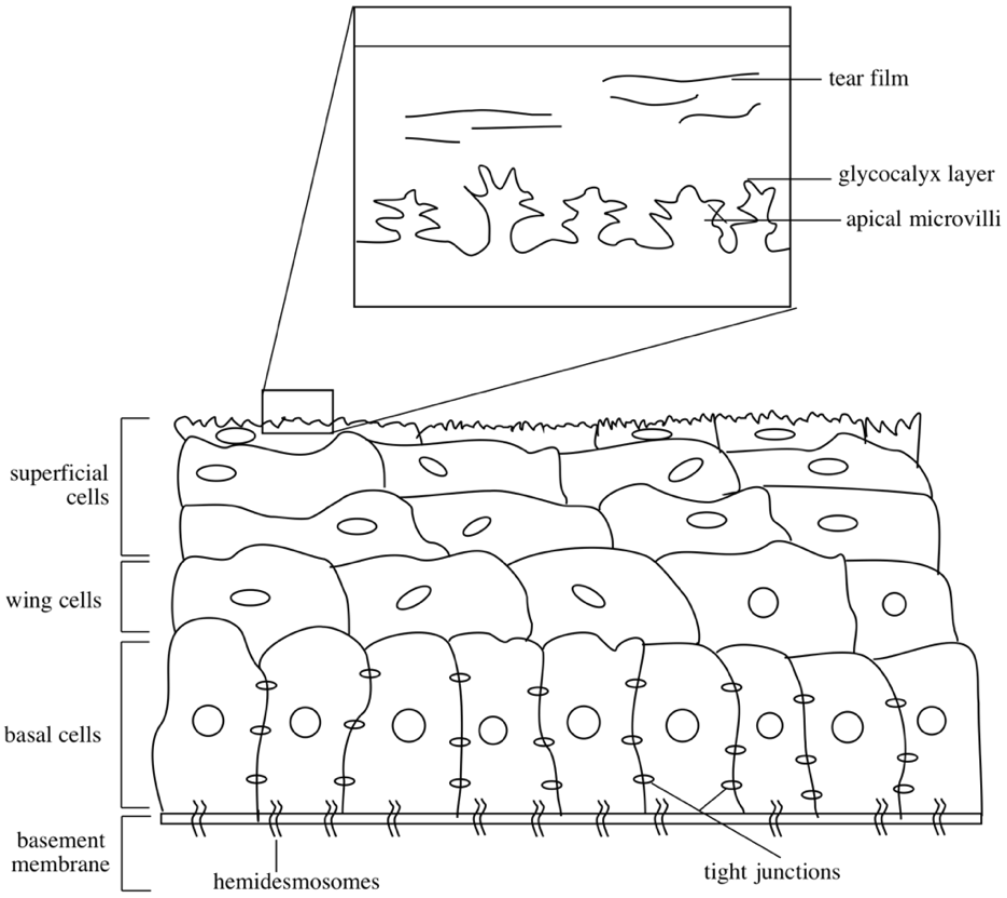


**Figure 2.** Cross sectional view of the layers of the corneal epithelium. Image reproduced with permission from [1].

Corneal epithelial cells live for approximately 7-10 days, while the epithelium itself undergoes very rapid regeneration every 3-10 days in order to maintain health, transparency and smoothness. The most superficial layer of the epithelium consists of 2-3 layers of flat polygonal cells that maintain the adhesion of the tear film's mucinous layer to the cell membrane. The surface area of this contact is made larger by the microvilli and microplicae present on the polygonal cells. As the superficial layer of the epithelium, these cells are anchored together via tight junctions in order to prevent agents from entering deeper layers of the cornea. Similar to this superficial layer, the subsequent 2-3 layers are composed of flat cells which are anchored by tight junctions for further protection[1].

The most basal layer of the epithelium is comprised of a single layer of columnar epithelial cells with a height of approximately 20μm. These cells are anchored to the basement membrane via hemidesmosomes. The basement membrane is approximately 0.05μm in thickness and composed of type I[14] and type IV collagen and laminin. Similar to limbal stem cells and transient amplifying cells, the cells of the basal epithelium layer are also capable of mitosis, differentiating into wing and superficial cells[28].

#### *2.1.1.1. Maintenance of the Corneal Epithelium*

Limbal epithelial stem cells (LESC) are the cells responsible for the maintenance and regeneration of the corneal epithelium[29]. The limbus is the barrier that separates the cornea from the conjunctiva[30,31]. These cells have an unlimited capacity for proliferation until they divide and give rise to early transient amplifying cells in the peripheral corneal epithelium[24]. There are several models that suggest how the limbal stem cells are maintained within the limbus. One such model suggests that following stem cell division, one daughter cell can either return to the original niche or migrate to a less favourable niche that allows it to retain its undifferentiated state as well as its stem cell characteristics. Subsequently these cells can either enter the differentiation pathway to eventually become corneal epithelial cells or remain undifferentiated (Figure 3)[30].

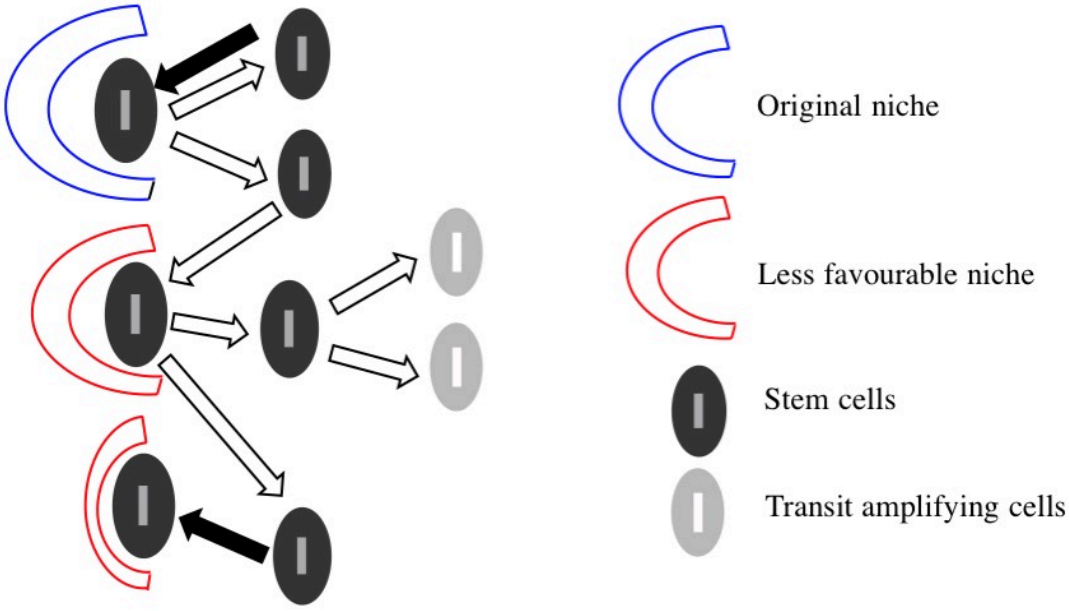


**Figure 3**. Stem cell niche hypothesis. Image adapted with permission from [2].

The turnover of corneal epithelial cells can be explained by the XYZ hypothesis. This states that the cells of the basal layer of the corneal epithelium will undergo mitosis (X), where the daughter cells will move upwards, differentiating into wing cells and eventually superficial cells. The newly differentiated basal cells from the limbus will migrate (Y) towards the centre of the cornea at a rate of approximately 120μm/week. The proliferative potential of transient amplifying cells diminishes as they migrate to the central cornea and become more mature transient amplifying cells [32]. Finally, the existing superficial epithelium is shed (Z) and replaced by the new layer[3].The speed of this cycle as well as the number of replications by the transient amplifying cells can be increased in response to injury or disease[33]

### *2.1.2. Bowman's Layer*

The second most anterior layer of the cornea is Bowman's layer or membrane. It is an acellular, nonregenerative, collagenous layer that is the condensation of the stromal layer[1,34–36]. Electron microscopy reveals that this layer is composed of randomly oriented and striated collagen fibrils, predominantly type I and III[37]. In normal eyes, it is 18.7±2.5μm in thickness,

and the thickness gradually decreases from the superior temporal region to the inferior nasal region , opposite to that of the corneal epithelium[38]. Although the overall function of this layer is relatively unknown, it is thought to play a role in maintaining the structure of the cornea. It may also act as a barrier that prohibits traumatic contact between the epithelium and the stroma, allowing for stromal healing to be rapid and maintains corneal transparency[39]. Due to its acellular composition, it acts as a biological barrier that prevents viral infection[40].

### *2.1.3. Stroma*

The majority of the cornea's thickness is provided by the stroma. This layer is shown in Figure 4. It is primarily composed of collagen, proteoglycans, glycoproteins and cells[22]. Collagen fibers (predominantly type I, III and V) are arranged in bundles known as fibrils in parallel layers known as lamellae, of which there are approximately 20 to 250 in human corneas. Each layer is distinct, with deeper layers being more organized than superficial layers. The overall organization of these layers is responsible for the cornea's transparency, mechanical strength and reduction in light scatter[1].

The collagen fibrils are surrounded by proteoglycans. Stromal proteoglycans are composed of a leucine protein core with a linkage region that allows for the covalent attachment of oligosaccharides and glycosaminoglycans[22]. These cores contain keratin sulphate glycosaminoglycans, which form the proteoglycans lumican,[41] keratocan [42] and mimecan[43]. These proteoglycans play a role in maintaining the ultrastructure of the stroma, such that when corneal scarring occurs, these proteoglycans are altered, with null mutations in the lumican proteoglycan resulting in corneal opacification.

At the cellular level, the stromal layer is primarily composed of keratocytes. Found in the anterior portion of the stroma between the collagen layers, their role includes maintaining the

extracellular matrix environment, synthesizing collagen, glycosaminoglycans and metalloproteases, which all contribute to the maintenance of stromal homeostasis. Furthermore, these cells also contribute to the transparency of the cornea since they contain proteins known as crystallins[44]. Finally, and most importantly, keratocytes respond to corneal injury by transforming into phenotypes that are specialized for repair[45].

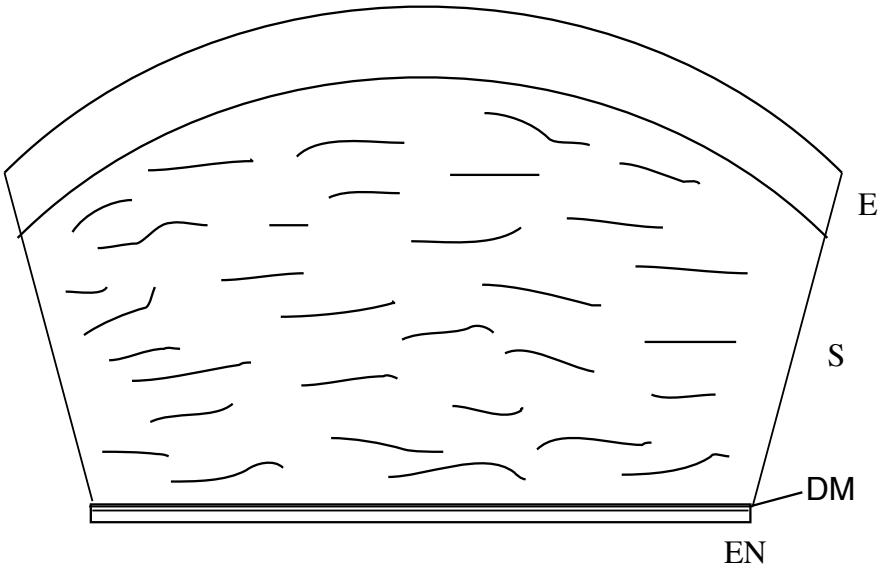


**Figure 4.** Illustration of the corneal stroma (S) in reference to the epithelial (E), Descemet's membrane (DM) and endothelial (En) layers. Image reproduced from [3].

### *2.1.4. Descemet Membrane*

Descemet membrane is a basement membrane, and therefore comprised of extracellular matrix biomolecules such as proteins and glycosaminoglycans[46]. The structure and composition of this layer varies throughout different developmental stages, increasing in thickness from birth (3μm) to old age (~10μm). From 12 to 16 weeks after conception, the anterior region of the membrane is deposited, and a striated pattern, known as the anterior banded layer, begins to form. This layer is composed of primarily type IV and type VIII collagen. A hexagonal lattice structure begins to arise due to the assembly of two polypeptide chains, α1 and α2, from type VIII collagen[47]. Mice that lack the genes for both of these polypeptide chains do not display this

banded pattern in their Descemet's membrane. Instead, the membrane is thinner and they display a lower endothelial cell count, which suggests that the anterior banded layer is crucial for the proliferation of endothelial cells[48].

Near birth, the secretion of type VIII collagen by endothelial cells decreases, and they shift to a non-proliferative state. Meanwhile, secretion of type IV collagen persists. Therefore, Descemet's membrane produced from this point does not possess a banded pattern and is known as the posterior non-banded layer.

### *2.1.5. Endothelium*

The most posterior layer of the cornea is the endothelium. This is a honeycomb-like monolayer, as seen in Figure 5. It is involved in the maintenance of corneal clarity by preventing hydration of the stroma thus preventing corneal swelling (edema). At birth, this layer is approximately 10μm thick and consists of a flattened layer of cells that fuse with the cells of the trabecular meshwork. These cells continue to flatten throughout life until they reach an approximate thickness of 4μm in adulthood[1]. There is a high density of Na+, K+-ATPase pumps within the lateral membranes, and the basal surface possesses hemidesmosomes that allow for the adhesion of the layer to Descemet membrane.

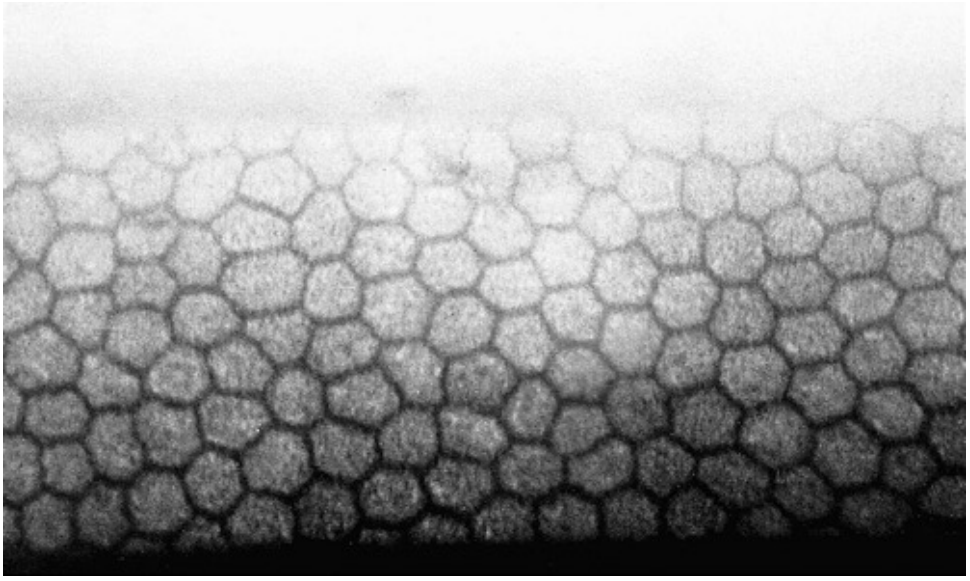

**Figure 5**. Specular micrograph depicting healthy endothelium with uniform cell sizes and a hexagonal array. Image reproduced with permission from [1].

Endothelial cell density begins to decline from the age of 20, continuing to approximately age 80. In this span of time, cell density may decrease from 400 to 1400 cells/mm$^2$. The central endothelial cell density is known to decrease by 0.6 per year in healthy corneas[49]. If cell densities drop below 500 cells/mm$^2$, then individuals may be at risk of corneal edema, since the number of cells is insufficient for maintaining the cornea in a dehydrated state[1].

### *2.2. Corneal Wound Healing*

Since the cornea is the most anterior surface of the eye, it is very susceptible to insult and injury due to its exposure to the external environment. The corneal epithelium undergoes constant renewal and regeneration approximately every 7 to 10 days, as epithelial cells are constantly shed and replaced by new cells[50,51]. Essentially, the healing process consists of cell migration, cell proliferation and cell adhesion. The level of involvement of each process will be dependent on the size and depth of the wound[23].

Wound healing begins with the latent phase, which takes place approximately 4 to 6 hours following injury. During this time, wound size will increase due to shedding of necrotic

cells and the retraction of cells found at the edge of the defect. Also, during this phase, intracellular synthesis of structural proteins is upregulated and all hemidesmosomal attachments between basal cells and the basal membrane dissipate up to 70μm from the edge of the wound, and those attachments that are at a distance of approximately 200μm from the wound edge are reduced. Superficial cells of the epithelium are desquamated, causing them to lose their columnar appearance, leading to a thinning of the epithelium at the wound to approximately 2-3 layers. These cells begin to fold, forming filopodia or lamellipodia processes that extend over the wound surface. Additionally, glycoproteins such as fibronectin and fibrinogen increase over the wound surface up to 8 hours following injury.

Cell migration begins during the linear healing phase. The formation of the filopodia and lamellipodia processes represents the beginning of cell migration, in which actin filaments within the cells are rearranged and synthesis of proteins and glycoproteins is upregulated. The covering of the wound by the filopodia and lamellipodia proceeds until complete cellular coverage is achieved. Cell proliferation is responsible for re-establishing the normal thickness of the epithelium over the wound and migration of cells begins from the limbus and moves towards the central cornea.

The process of cell proliferation is responsible for restoring cell numbers and cell mass. Research has shown that a "mitosis wave" occurs from the periphery to the centre until normal thickness of the epithelium is restored and the wound is healed. The cells mainly participating in the proliferation process are basal epithelium cells, which are derived from the limbal basal epithelium. This is a source of stem cells that migrate from the periphery initially as transient amplifying cells and eventually differentiate into corneal epithelial cells upon reaching the

central cornea (Figure 6). Due to the location of these cells, wounds that occur in the peripheral cornea heal faster than those near the centre.

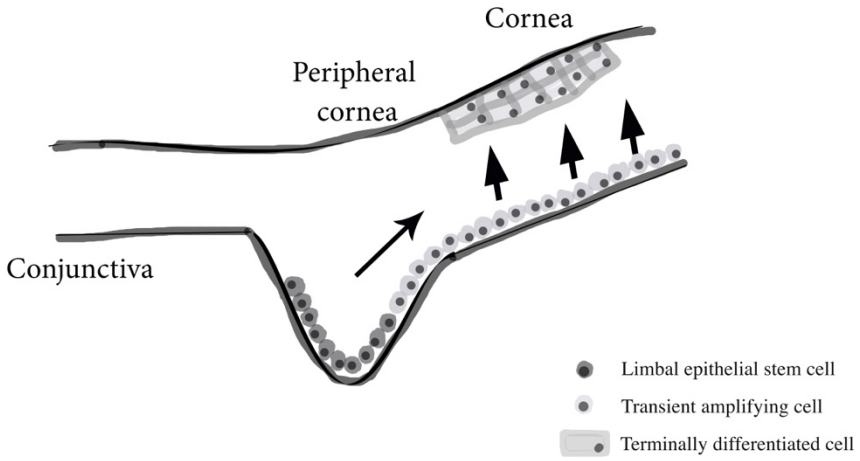


**Figure 6.** Illustration depicting the migration of limbal epithelial stem cells from the limbus, towards the central cornea where they become terminally differentiated cells or corneal epithelial cells. Image reproduced from [4]

After cells have proliferated and migrated over the wound site, healing is not complete until the newly generated epithelium is then anchored to the underlying tissue. Transient attachments are formed and dissociated in order to draw the cells forward towards the wound, and more permanent attachments are formed when complete coverage of the wound occurs. As previously mentioned, extracellular matrix proteins such as fibronectin, fibrinogen/fibrin, tenascin and laminin appear soon after wounding occurs. Cells migrating from the limbus towards the central cornea form adhesion plaques, which are specialized cytoskeletal complexes consisting of intracellular stress fibres, plasma membrane and extracellular substrate. Filopodia and lamellipodia are the first to establish focal contact and help to provide anchorage while contractile mechanisms found within the cell work to draw cells forward. Fibrin and fibronectin proteins trigger the release of plasminogen activator by the epithelial cells, which in turn is converted to plasmin that lyses the adhesions and allows the cells to form new ones, ultimately

advancing them forward. This process is halted upon closure of the wound in a process known as contact inhibition, at which time permanent hemidesmosomal attachments are formed. This process may be prolonged if the basement membrane was also damaged during wounding, as migrating cells must secrete basement membrane before permanent attachments can form[23,52,53].

## *2.3. Current Treatments for Corneal Injury*

### *2.3.1. Stem/Epithelial Cell Transplantation*

As an alternative to corneal donors, stem cell transplantation may also be an option for some patients. The transplantation of stem cells over the recipient's limbus involves the use of amniotic membrane, on which limbal donor is cut and glued using fibrin glue[54]. It is suggested that amniotic membrane can promote reepithelialisation, inhibit angiogenesis and decrease the occurrence of inflammation followed by fibrosis[33]. Although successful and still currently in use, amniotic membrane is associated with several drawbacks, such as its biological availability, the variation amongst donors, viral agent transmission and, most importantly, its lack of transparency, which is an essential factor when considering ophthalmic biomaterials[55,56]. Furthermore, amniotic membrane is insufficient to treat partial limbal stem cell deficiency.

In case of bilateral disease, donor tissue can be used for a direct transplant or cultured prior to transplantation. Surgeons have also developed a technique called cultivated oral mucosal epithelial transplantation (COMET). This involves collecting the cells that line the patient's mouth and culturing them so that they may be transplanted into the patient's eye. Although this is a readily available source that avoids the need for immunosuppression, the epithelium does not remain clear for as long as limbal epithelial cells[9].

### *2.3.2. Keratoprosthesis*

A kerataprosthesis (KPro) is a corneal substitute for the restoration of vision within patients suffering from corneal disease or degeneration[10]. These must be constructed with materials that are transparent, capable of maintaining the barrier function of the cornea, non-biodegradable, and oxygen- and nutrient-permeable[57]. Additionally, it is essential that these materials are able to promote migration, and proliferation of the remaining host corneal cells, so that corneal functioning is restored.

In order to achieve this, a KPro can assume one of two main types of designs. The first, less commonly used design, is a collar-button device[8]. This involves the use of a front and back plate, and a titanium locking c-ring. The front plate includes a stem which functions as the optical component of the device (Figure 7a)[5]. The second, more commonly used design, is the core and skirt model (Figure 7b). The optical core is ideally constructed from a flexible and transparent material, whereas the skirt is porous, flexible and hydrophilic. The skirt is the component that is primarily responsible for keratocyte adhesion and spreading. However, it is possible for both of these components to be composed of the same material. The core and skirt are joined together by an interpenetrating network (IPN).

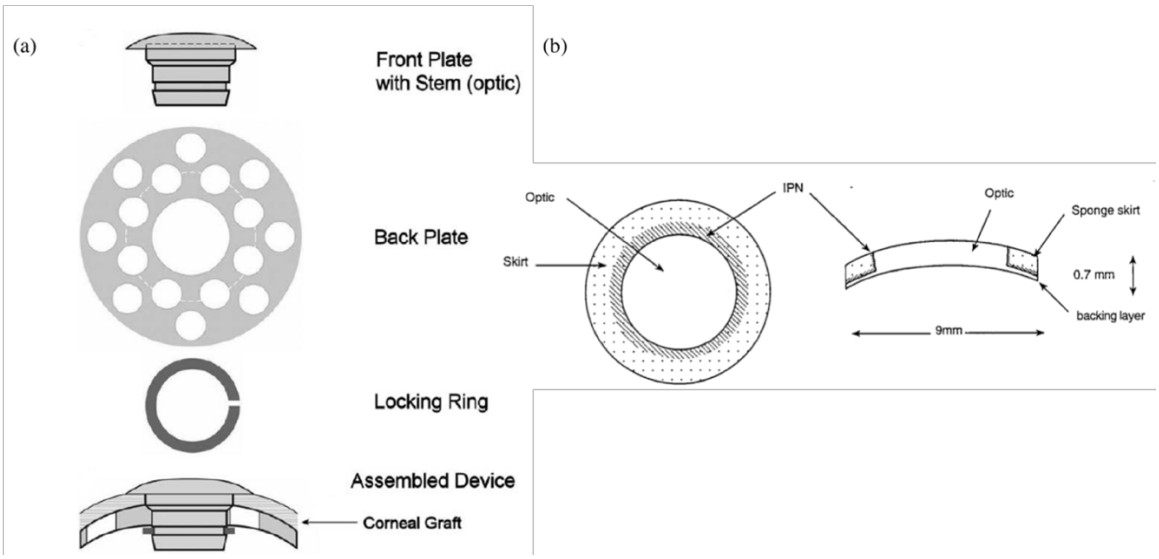


**Figure 7.** The two possible designs for a keratoprosthesis device. (a) Collar-button device: consisting of an optical front plate, back plate and locking ring. Image reproduced with permission from [5] (b) Core and skirt device: consists of a porous sponge skirt and optical core, connected by an interpenetrating network (IPN). Image reproduced with permission from [6].

### *2.4. Tissue Engineering of Corneal Scaffolds*

The material chosen to synthesize a KPro device must satisfy several requirements. These requirements include transparency, an appropriate refractive index, strength to maintain the barrier function of the cornea, permeability to oxygen and nutrient transfer and cytocompatibility[58]. The Boston KPro and AlphaCor KPro utilize poly(methyl methacrylate) (PMMA) and poly(2-hydroxyethyl methacrylate), respectively. Both of these materials possess characteristics that render them as suitable candidates for corneal replacement, whether by the device itself or with the incorporation of a donor corneal graft. However, tissue engineering serves to develop materials that can replace damaged tissues by mimicking their properties or promoting tissue repair. Therefore, it is vital for these materials to mimic the physical structure/topography of these tissues, as well as incorporate biological elements such as proteins and growth factors[12].

There are several surface modification techniques that have been used to render surfaces more favourable for cellular attachment, or in order to prepare them for further treatment. In order to best promote re-epithelialization by remaining host corneal cells (or cells that have been seeded onto the surface in vitro), the synthetic material may be modified in order to present a surface that is favourable for cell adhesion and proliferation[57].

A material's surface properties can be altered through surface-attached polymers. These polymers may tailor properties such as wettability, friction, lubrication, adhesion and biocompatibility. While enhancing these surface properties, the bulk properties of the material are minimally affected. Furthermore, these surface-confined polymers are mechanically and chemically robust and capable of being grafted onto every surface of varying thickness, chemical composition and in a wide variety of co-polymer blocks[20,21,59,60].

### *2.4.1. Surface Grafting Techniques*

The technique used to graft polymer brushes onto the surface can greatly affect the material's surface architecture, and therefore the surface properties. There are two main ways to deposit polymers onto a material's surface: physisorption and covalent attachment. In the case of physisorption, adhesive functional groups found within the polymer chain simply adsorb to the surface non-covalently. On the other hand, covalent attachment to a surface is much more stable and desirable for biomedical applications. Within covalent attachment, there are two approaches that are generally used: "grafting to" and "grafting from", as illustrated in Figure 8.

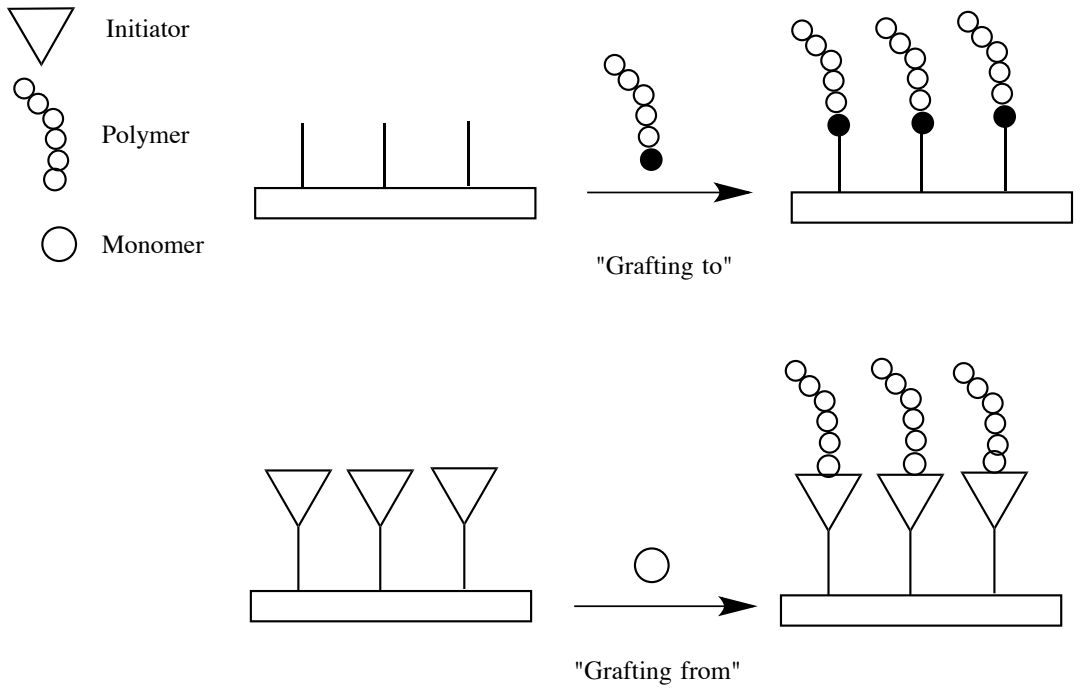


**Figure 8.** Illustration depicting the difference between the two approaches for grafting polymer brushes onto a surface.

#### *2.4.1.1. "Grafting to" Approach*

This approach involves grafting of an end-functionalized polymer onto a substrate with reciprocal reactive groups on its surface[20]. These polymers can be synthesized through several polymerization and copolymerization techniques. This includes controlled and conventional radical and anionic polymerization. This approach presents several advantages including its simple experimental synthesis and the ability to incorporate well-defined brushes to the material's surface[20,59].

However, this method also presents several disadvantages. Reactive sites present on the material's surface may be sterically crowded by polymers brushes that have already been adsorbed. Additionally, the thickness of the polymer brush layer obtained on the surface is limited to approximately 1-5 nm[61]. This is because the polymers that are to be grafted onto the surface must diffuse through the polymer film in order to reach the reactive sites for covalent

attachment. As the thickness of the polymer brushes increases, so does the thickness of the polymer film[20,21,59,62]. Therefore, the grafting density obtained through this approach is low and insufficient for several applications. Due to these significant drawbacks, the "grafting from" method was developed and has gained considerable attention within surface modification applications.

#### *2.4.1.2. "Grafting from" Approach*

To overcome the drawbacks presented by the aforementioned method, the "grafting from" technique, also known as surface-initiated polymerization (SIP), may be used. Rather than using an end-functionalized polymer, the material's surface is modified with an initiator monolayer, from which direct polymer chain growth can occur. This bypasses the diffusion barrier that is seen in the "grafting to" approach as now only the monomer must reach the reactive sites on the material's surface and the reactive sites are not on the underlying substrate but rather are on the end of the grafted layer. Therefore, thicker polymer brushes and a greater grafting density can be achieved through this technique[21,59,63]. The initiator monolayers can be formed on any surface so long as the anchoring method chosen is appropriate for the material[21].

In addition to the grafting approach chosen, the polymerization technique for the construction of the polymer brushes can also affect surface functionalization and this can be dependent on the initiator monolayer deposited on the surface. A wide variety of polymerization techniques can be used to form the polymer brushes. This includes but is not limited to conventional free-radical polymerization and controlled living radical polymerization[21]. Although both of these can efficiently produce polymer brushes tethered to a material surface, the architecture of this layer will differ depending on the technique used.

#### *2.4.1.3. Conventional Free-Radical Versus Controlled Living Radical Polymerization*

Within industry, conventional free-radical polymerization (CFRP) has been used to manufacture products such as plastics, rubbers and fibers[64]. In addition to having mass production capabilities, this form of polymerization allows for: the use of a wide variety of monomers to be polymerized with relatively simple reaction conditions (e.g., only the absence of oxygen in some cases), tolerance to water and other impurities and, can occur at a wide temperature range from 0 to 100° C. However, this polymerization technique does not allow for control of the molecular architecture of the polymer brush[65]. The CFRP mechanism involves slow initiation and rapid propagation and termination, which therefore produces non-uniform, high molecular weight polymer chains.

Alternatively, controlled living radical polymerization (CLRP) is a technique that allows for the preparation of well-defined polymer brushes with controllable molecular weights, architecture, composition and low polydispersity[21,60,63,65]. Within CLRP, one of the most successful methods is atom transfer radical polymerization (ATRP). This form of polymerization utilizes a transition metal halide catalyst, a nitrogen-based ligand, the monomer of interest and a solvent (Scheme 1).

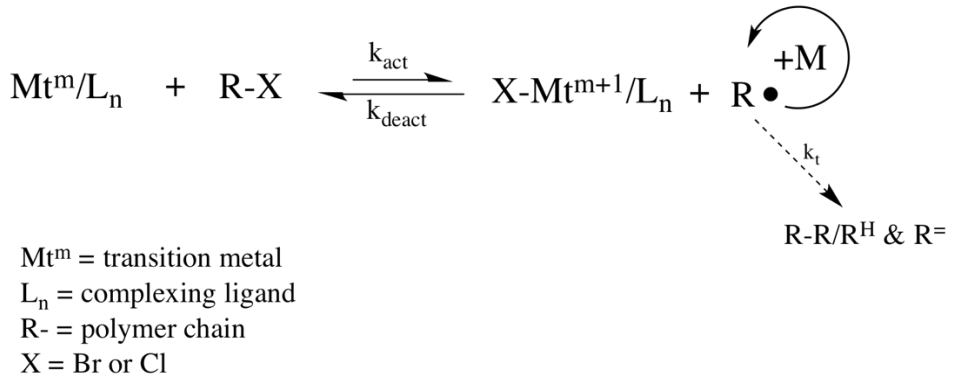


**Scheme 1**. Mechanism of Atom Transfer Radical Polymerization (ATRP). Image adapted from: http://www.cmu.edu/maty/chem/fundamentals-atrp/atrp.html.

The transition metal and ligand complex create a reversible equilibrium between the growing radicals ($P_n$*) and the dormant species ($P_n$-X, where X is Br or Cl and $P_n$ is the polymer chain), which is usually an initiating alkyl halide. The dormant species may react with an activator or deactivator species. The activator ($Mt^m/L_n$, where Mt is the transition metal in the *m* oxidation state and $L_n$ is the ligand) will react with the dormant species in the lower oxidation state to form radicals with the rate constant of activation ($k_{act}$). In the reverse direction, the deactivator ($X\text{-}Mt^{m+1}/L_n$) will react with the propagating radicals in the higher oxidation state to re-form the dormant species with a rate constant of deactivation ($k_{deact}$). Ultimately, the dormant species will go on to regenerate the activator. Polymer chain growth occurs through the addition of the monomer of choice (M) to the radicals at a rate constant of propagation ($k_p$), while termination occurs through disproportionation or recombination through the rate constant of termination ($k_t$). The concentration of propagating radicals is sufficiently lower than that of the dormant species, and so the proportion of chains undergoing termination will be approximately <5%, resulting in the formation of well-defined polymer chains[66].

Both CFRP and CLRP can be used with a wide variety of commercially available initiators, monomers and solvents[64,67]. Furthermore, both of these polymerization techniques have been used for the development of biomaterials of different functionalities. The CFRP

technique has been used to manufacture polymers used to construct cardiovascular stents[68] as well as "self-healing" polymers[69], however the addition of polymer brushes using this method has not been widely explored due to the lack of control over the growing polymer's architecture. Therefore surface-initiated ATRP (SI-ATRP) has been more widely investigated for the construction of biomaterials. The highly controllable nature of this technique can create well-defined polymer brushes out of monomers that act as mitogens to cells and therefore provide opportunities for regeneration or replacement of damaged tissues and organs.

### *2.5. Boronic Acids*

Boronic acid (Figure 9a) has been used within a variety of biomedical applications, most notably for their incorporation into saccharide-responsive hydrogels, sensors and nanomaterials that are ultimately used for type-1 diabetes detection and treatment. However, boronic acids have also been implicated within cellular applications. Most notably, it has been reported that they may support cell cultures, allow for cell capture and release, as well as for mediating cellular interactions with biological and synthetic materials[18].

The interactions between boronic acids and cells is due to their capability of boronic acids to bind to glycoproteins at cell surfaces. As well, the adsorption of glycoproteins that mediate cell adhesion such as fibronectin and vitronectin can occur[70]. This is possible due to their mucoadhesive properties, as well as the stable covalent bond that may be formed between boronic acids, especially phenylboronic acids (PBA), (Figure 9b) and 1,2- and 1,3-diols. These compounds are often found as functional groups on several saccharides [71–75].

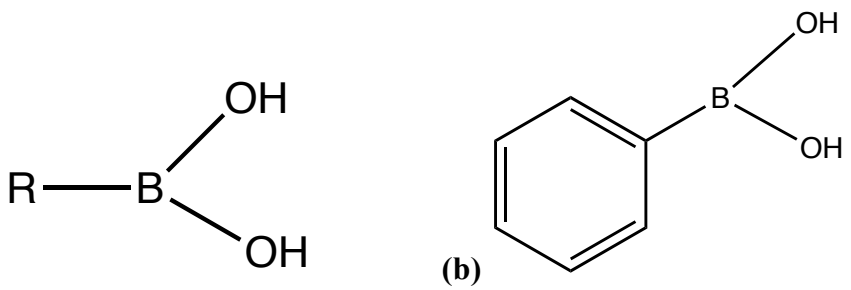


**Figure 9. (a)** Chemical structure of boronic acid. **(b)** Chemical structure of phenylboronic acid (PBA).

In aqueous media, a boronate ester may form when boronic acid reacts with a hydroxide ion. This indicates that boronate formation is dependent on the pH of the solution. When the pH of the solution is equivalent to the p*K*a of phenylboronic acid (approximately 9), the concentrations of boronic acid and the boronate ester are equivalent. In terms of saccharide binding, it is the boronate ester form that is vital for diol interactions (Scheme 2) [71,76]. In a solution that is neutral or weakly alkaline, only a limited amount of the boronate ester form exists. When a saccharide is added to the solution, the p*K*a value decreases and the boronate ester may bind to the hydroxyl groups present on the sugar. This can be explained by the theory described by Lorand and Edwards[77]. When a sugar is added, the boronate form binds the hydroxyl (OH) groups present on the sugar in order to form a cyclic ester, which leads to the consumption of the boronate form. In order to maintain acid-base equilibrium, the boronic acid form changes into the boronate form. Overall, the addition of a sugar leads to a decrease of the boronic acid form and ultimately to the decrease of the apparent pKa.

Conversely, boronic acids can release captured cells through an increase in pH levels as well as through the addition of a saccharide such as glucose[78]. These cell detachment methods eliminate the need for trypsinization, which is known to cause cell damage, through the digestion of cell attachment proteins found in the membrane[79].

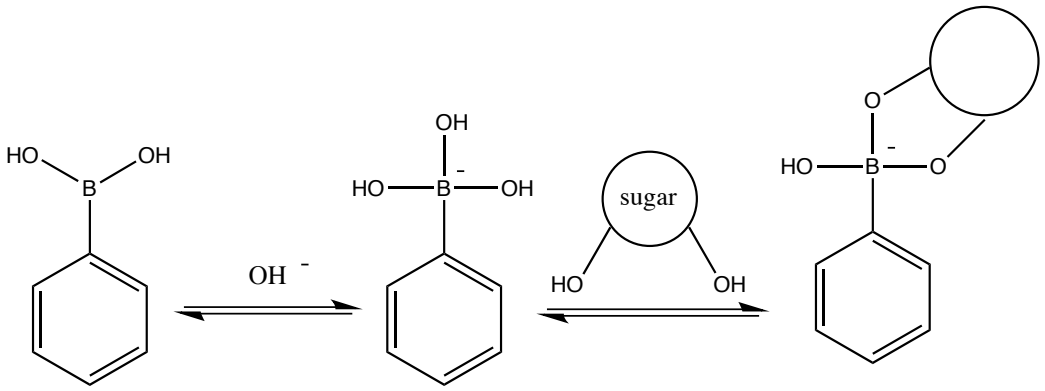


**Scheme 2**. Equilibriums of phenylboronic acid and saccharides.

PBA has been reported to interact with sialic acid (SA), which is a negatively charged monosaccharide that is found on the terminal end of carbohydrate chains, extending from cell membrane lipids and glycoproteins[70,74,80]. These SAs have been shown to play a major role in the mediation or modulation of cellular interactions, including cell adhesion, signal transduction as well as immune responses. The most common SA found in mammalian cells is *N*-acetylneuraminic acid (Neu5Ac), particularly at a physiological pH of 7.4[70,81] (Figure 10). The interaction between PBA and SAs has been reported mainly in cancer cells, such as MCF-7, due to the overexpression of SA in the cell membrane. However, SAs are found in normal amounts in the cell membranes of other cell types including epithelial cells, endothelial cells as well as fibroblasts[80,82].

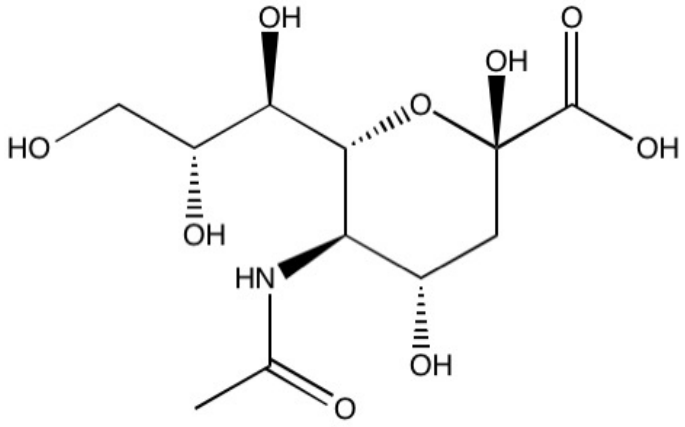


**Figure 10**. Chemical structure of N-acetylneuraminic acid (Neu5Ac).

There has been a considerable amount of work regarding the surface modification of materials with phenylboronic acid for cell capture and release [19,74,78,79]. However, the grafting of phenylboronic acid through conventional free radical and controlled living polymerization techniques has not been explored for the application of synthetic corneal scaffolds.

### *2.6. Scope of Work*

The overall objective of this thesis is to synthesize a corneal scaffold that can act as a surrogate for a diseased or degenerating cornea. The synthetic scaffold will be modified in order to enhance cytocompatibility and promote cell adhesion and proliferation, with the ultimate goal of regenerating the cornea through the augmentation of remaining host corneal cells.

pHEMA is a cytocompatible material that possesses ECM-like characteristics and can absorb water for hydration. In this work, its cell-repelling properties are altered through surface modification with phenylboronic acid. Phenylboronic acid is grafted onto the surface via CFRP and ATRP such that it is available for direct covalent bonding with carbohydrates found on the cell surface.

## 3. Materials and Methods

### *3.1. Materials*

Prior to use, 2-Hydroxyethyl Methacrylate (HEMA) (99%, Sigma-Aldrich) and Ethylene Glycol Dimethacrylate (EGDMA) (98%, Sigma-Aldrich) were passed through a column containing inhibitor remover to remove the inhibiors hydroquinone and monomethyl ether hydroquinone (MMEQ) (Sigma-Aldrich). Triethylamine (TEA) ≥ 99%, anhydrous dichloromethane (DCM) ≥ 99.9%, anhydrous toluene ≥ 99.8%, anhydrous pyridine ≥ 99.8%, 2,2-Bipyridyl (bpy) and methacryloyl chloride (90%) were purchased from Sigma-Aldrich and used as received. Acetonitrile (ACN), methanol (MeOH), 2-proponaol, N,N-dimethylfomamide (DMF) (reagent grade, Caledon Laboratories) and anhydrous ethanol (EtOH) (Commercial Alcohols) were used as received. Recrystallized 2,2'-azobis(2-methylproprionitrile) (AIBN, 99%) and 3-(acrylamido)phenylboronic acid (PBA, 98%) were purchased from Sigma-Aldrich and used as received. Cu(I)Br ≥ 97% was purchased from Sigma-Aldrich, stirred in glacial acetic acid overnight, rinsed with ethanol and diethyl ether, and stored under nitrogen to prevent oxidation[83]. For cell culture, Fetal Bovine Serum (FBS), penicillin/streptomycin solution, 1x trypsin-EDTA (0.05%) and Dulbecco's Modified Eagle's Media (DMEM) containing L-glutamine, sodium bicarbonate and glucose (4500 mg/L) were purchased from Sigma-Aldrich, and were used as received. Cell Proliferation Kit I (MTT) was purchased from Sigma-Aldrich and was used as received. Mouse embryo NIH 3T3 cells (50,000 cells/vial) were purchased from the American Type Culture Collection (ATCC) and were used as received.

### *3.2. Synthesis of Unmodified pHEMA Scaffold*

The unmodified pHEMA hydrogel was synthesized through the addition of 4000 mg of the hydrophilic HEMA monomer (96 wt%), 120 mg of an EGDMA crosslinker (3 wt%), and 40 mg of the photoinitiator Irgacure® 184 (1 wt%) in a 20 mL glass vial and stirred until complete dissolution. This monomer solution was injected into a mold composed of a 1 mm thick Teflon spacer between two acrylic plates bolted together. Polyester sheets lined the Teflon spacer to prevent adhesion of the polymer. Subsequent to the monomer injection, the mold was placed into a 400 W UV chamber (Cure Zone 2 Control-cure, Chicago, IL, USA) for polymerization at a wavelength of 365 nm for 15 minutes. Following polymerization, the polymer was removed from the mold and placed into a beaker containing 500 mL of Mili-Q water for 24 hours to soak and remove any unreacted monomer or other residual components. Circular discs 1 cm in diameter were then punched from the polymer film. The discs were dried in a vacuum oven for 24 hours and placed in a 37°C oven until use.

### *3.3. Surface Grafting of APBA to pHEMA Scaffold via CFRP*

#### *3.3.1. Step 1: Surface Methacrylation of pHEMA (Vinyl Incorporation)*

In order to graft PBA on the pHEMA surfaces, the surface chemistry must be altered to allow for attachment. This requires the replacement of the hydroxyl groups on the pHEMA surface with vinyl groups. Thus, approximately 10 samples of unmodified pHEMA discs were placed in a 20 mL glass vial with a magnetic stir bar and covered with tinfoil due to the photosensitive nature of the reaction. Next, anhydrous dichloromethane (DCM) was de-aerated under a stream of nitrogen for 5 minutes and 10 mL of this solvent was transferred to the vial. To this solution, 2 mL of triethylamine (TEA) were added to the vial, followed by 0.4 mL of methacryloyl chloride (MACL) in a dropwise manner. The solution was stirred at a speed of 550

rpm at room temperature and the reaction was allowed to proceed for four hours. Once a transparent red solution was observed, the samples were removed from the reaction vessel. The discs were rinsed three times with a 6 mL solution of anyhydrous ethanol:acetonitrile (1:1) and placed to dry in a vacuum oven for 24 hours. Lastly, they were placed in a 37°C oven until use (Scheme 3).

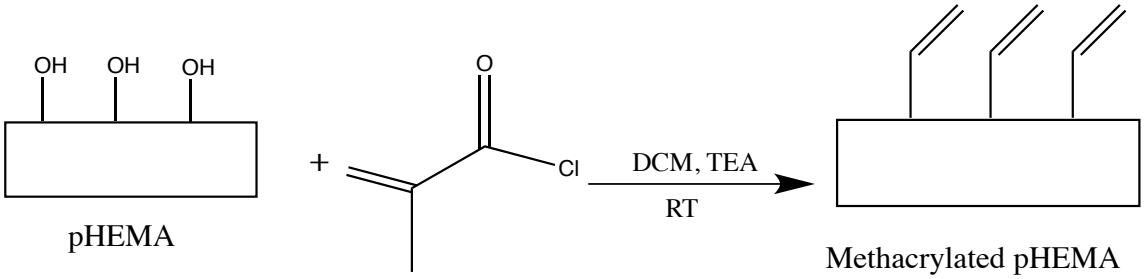


**Scheme 3**. Surface methacrylation of pHEMA.

### *3.3.2. Step 2: Incorporation of 3-(acrylamido)phenylboronic acid via Free Radical Polymerization*

As the discs possessed a favourable surface chemistry for binding, 3-(acrylamido)phenylboronic acid (APBA) could be attached via free radical polymerization (Scheme 4). The discs from step 1 (1.3.1) were placed in a 25 mL dry round bottom flask equipped with a magnetic stir bar and the flask was purged with nitrogen for 10 minutes. Then, 10 mL of acetonitrile:anhydrous ethanol (9:1) was added to the flask. The recrystallized thermoinitiator 2-2'-azobis(2-methylpropionitrile) (AIBN) was diluted with acetonitrile to a concentration of 50mg/mL, and 30 μL of this solution was added into the round bottom flask. Finally, 95 mg of 3-(acrylamido)phenylboronic acid was added to the flask, which was then sealed with parafilm. The solution was degassed by bubbling for 10 minutes in an oil bath at 70°C and stirred at a rate of 550 rpm. Following initial degassing, a nitrogen-filled balloon was attached to a 10 mL syringe with a 16G needle which was inserted into the reaction vessel, and

the reaction was allowed to proceed under these conditions for two hours. The discs were then removed from the flask and were rinsed twice with a 10 mL solution of anhydrous ethanol:acetonitrile (1:1) followed by 5 mL of Mili-Q water. The discs were dried in a vacuum oven for 24 hours and subsequently placed in a 37°C oven until further use.

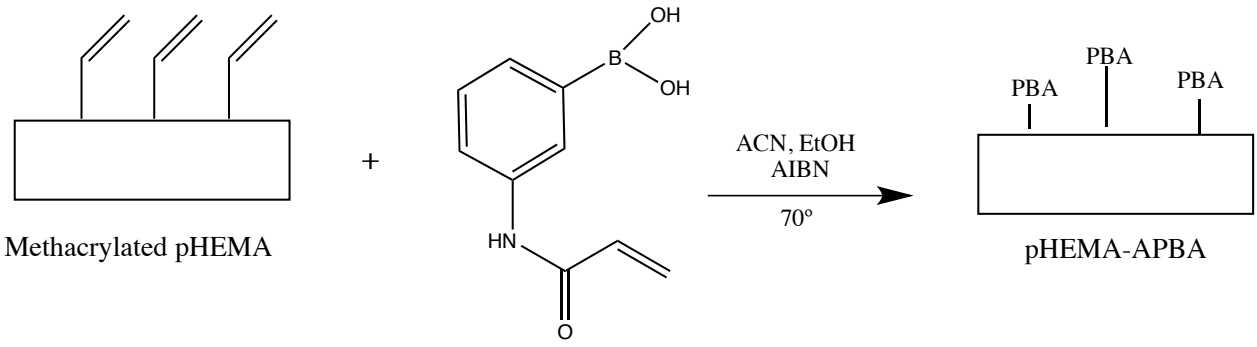


**Scheme 4**. Grafting of PBA on methacrylated pHEMA surface via free radical polymerization.

### *3.4. Surface Grafting of APBA to pHEMA Scaffold via ATRP*

#### *3.4.1. Surface Treatment of pHEMA Scaffold*

Prior to the growth of APBA brushes from the surface, reactive sites from which the polymer chains can grow must be attached onto the surface (Scheme 5). To a 50 mL round bottom flask equipped with a magnetic stir bar, 20 mL of aerated anhydrous toluene was added along with 15 pre-weighed unmodified pHEMA discs (0.97 g), and the vessel was sealed with parafilm. This solution was placed in an ice bath containing 100 g of sodium chloride (NaCl) and bubbled under a stream of nitrogen for 40 minutes. Pyridine (2.1 mL) was then added to the round bottom flask and the solution was left to stir at 650 rpm. In a separate vial, 4.08 mL of α-bromoisobutyryl bromide was added to 10 mL of toluene and mixed. The contents of this vial were then added to the round bottom flask in a dropwise manner. The ice bath was changed 3 times, and the reaction was allowed to continue overnight.

The following day, the discs were removed and washed three times with 10 mL of N,N-dimemethylformamide (DMF), followed by rinsing with 20 mL of Mili-Q water, and then the discs were left to soak overnight. The discs were removed, their surfaces were dabbed dry with a Kimwipe and they were left to air dry for 2 hours. Finally, the discs were placed in a vacuum oven overnight for complete drying and then transferred to a 37°C oven until further use.

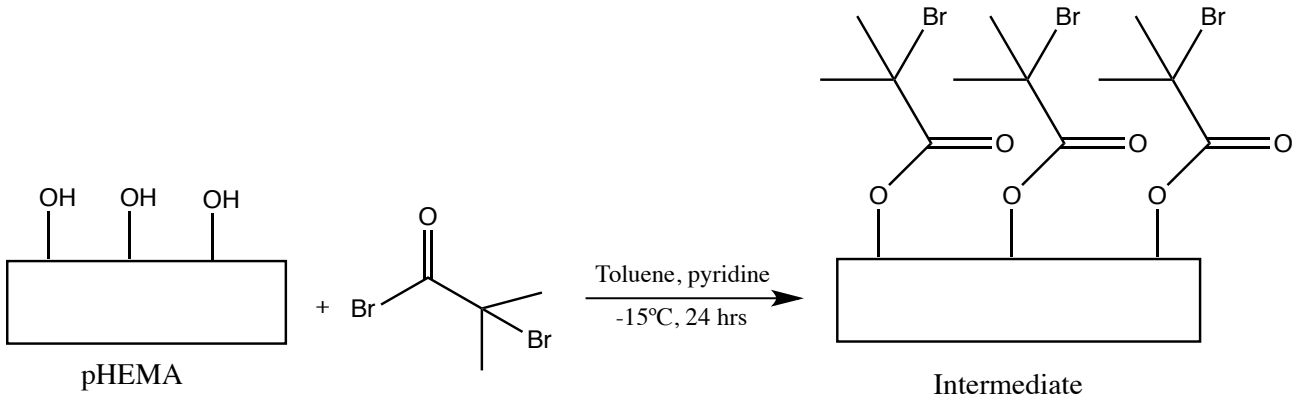


**Scheme 5**. Grafting of initiator onto pHEMA surfaces.

### *3.4.2. Incorporation of APBA onto pHEMA Surfaces via ATRP*

With reactive sites linked to the surface of the materials, the APBA monomer could be added to form polymer chains from these sites (Scheme 6). To a 25 mL one neck round bottom flask, 572.97 mg of APBA was added followed by 15 mL of ACN, 0.75 mL EtOH and a magnetic stir bar. After the dissolution of APBA, 16.97 µL of benzyl-bromo isobutyrate (BBIB) initiator was added and the flask was sealed with parafilm. The flask was then set in an ice bath and the solution was bubbled with nitrogen for 45 minutes. Following this, a nitrogen-filled balloon was attached to a 10 mL syringe with a 16G needle was inserted into the flask to allow for nitrogen protecting.

A 25 mL schlenk flask equipped with a magnetic stir bar was filled with 12 previously prepared surfaces (1.4.1) and 18.74 mg 2,2-Bipyridyl (bpy) ligand. The flask was then degassed under vacuum and backfilled with nitrogen a total of three times. Following nitrogen purging,

8.607 mg of $CuBr_2$ was added to the schlenk flask and the flask was sealed with parafilm. The flask was again degassed under vacuum and backfilled with nitrogen an additional three times. In the one neck round bottom flask, the previously prepared solution in the one neck round bottom flask was then transferred to the schlenk flask using an 18G long needle, and all openings on the schlenk flask were tightly sealed using parafilm. The flask was set in an oil bath at 70°C, and the mixture was allowed to stir for 24 hours. The reaction was stopped by the removal of the discs, and the subsequent washing with a 10 mL solution of methanol (MeOH) and Mili-Q water (1:1). Then, the discs were placed into a 10 cm petri dish for air drying. Once surfaces turned green, they were transferred to a vacuum oven to ensure complete dryness, and were placed into a 37°C oven until further use.

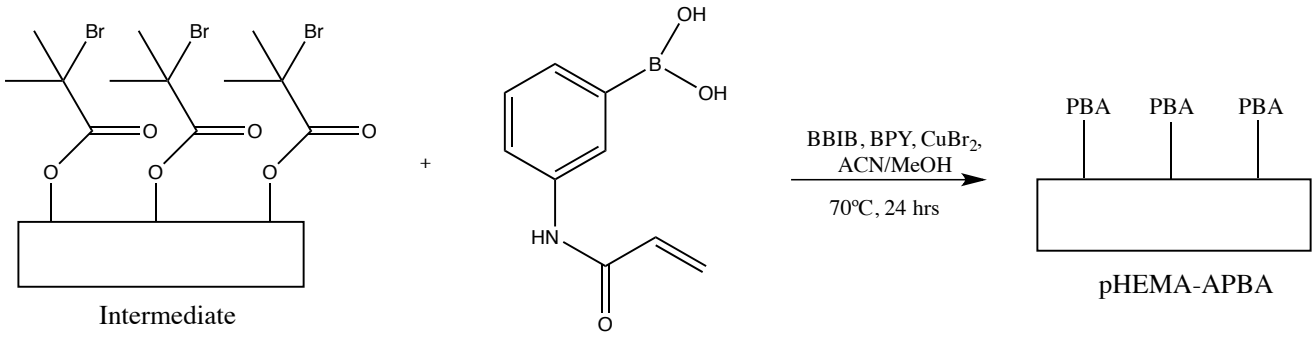


**Scheme 6.** Polymerization of the APBA monomer onto pHEMA surface.

### *3.4.3. Soxhlet Extraction of Copper from Surfaces*

The green colouration of the discs following the incorporation of APBA is an indication of the Cu (II) species on the surface. As this is toxic to the cells, a Soxhlet extraction is necessary in order to remove this residue from the surface. A 500 mL round bottom flask was equipped with a magnetic stir bar and filled with 300 mL of 2-propanol/$H_2O$ (70:30) The solution was placed into an oil bath at 100°C and stirred at 400 rpm. Pre-weighed discs (n=5) were placed inside the extraction thimble. The thimble was placed into the main chamber of the Soxhlet extractor,

which was placed on top the solvent flask. Finally, the reflux condenser was equipped with a water-in and water-out tube and was placed on the extractor. This arrangement allows for the evaporated solvent to travel up the distillation arm and into the condenser. The condenser will cool the solvent vapours and allow them to drip down into the main chamber of the Soxhlet where the discs are located. The temperature was gradually increased to 120°C in order to achieve a drop rate of approximately 1 drop/second. When the main chamber is full, it will empty via the siphon back into the round bottom flask. After the first cycle was completed, the extraction process was allowed to proceed for two hours. Following the final cycle, the column was disassembled and the extracted discs were left to air dry inside the thimble for 24 hours. Then, the discs were placed in a vacuum oven for 24 hours to ensure complete dryness, and stored in a 37°C oven until further use.

### *3.5. Polymer Characterization*

#### *3.5.1. Surface Chemical Composition*

After each surface modification step, the surface chemical composition was analyzed by Attenuated Total Reflectance-Fourier Transformed Infrared Spectroscopy (ATR-FTIR) using a Bruker Hyperion 3000 Microscope and Vertex 70 Bench and HTS Plate Reader. Furthermore, surface chemical composition was assessed by X-ray Photoelectron Spectroscopy (XPS). Prior to this, the discs were rinsed in ethanol:Mili-Q water (50:50) solution and dried in a nitrogen-purged glass vial. The spectra were generated using a Physical Electronics (PHI) Quantera II spectrometer equipped with an AI anode source for X-ray generation and a quartz crystal monochromator for focusing the generated X-rays. Low resolution spectra for boron and high-resolution scans for carbon were obtained at a 45° take off angle, using a dual beam charge compensation system for neutralization of all samples.

### *3.5.2. Surface Wettability*

The wettability of pHEMA and APBA-modified discs was assessed through contact angle measurements using the sessile drop technique with an Optical Contact Angle (OCA 35) high speed instrument. Prior to testing, surfaces must be sufficiently hydrated. Therefore, unmodified and APBA-modified pHEMA discs (n=5) were placed within Mili-Q water for 48 hours[84]. For testing, surfaces were gently dried with a Kimwipe to remove water on the surface and a 3 μL drop was dispensed onto the surface for measurement.

## *3.6. Cell Culture*

All protocols involving the handling of cells were performed in a level 2 biosafety cabinet using aseptic technique.

### *3.6.1. Cell Thawing*

Dulbecco's Modified Eagle's Medium (DMEM) was prepared through the addition of and Fetal Bovine Serum (FBS) (1:10 dilution) and penicillin/streptomycin (1:100 dilution). In a T75 sterilized tissue culture flask, 10 mL of DMEM was added and placed into the incubator (37°C, 5% $CO_2$) to equilibrate. Meanwhile, the cryovial containing mouse embryo 3T3 fibroblasts was removed from liquid nitrogen storage and placed into a 37°C water bath for approximately 2 minutes, until the crystals have melted.

### *3.6.2. Cell Seeding*

Immediately after cell thawing, 800 μL of the cell suspension was aspirated from the cryovial and dispensed into the tissue culture flask, along with 10 mL of DMEM. The flask was gently mixed in order to evenly distribute the cells. The flask was then placed into a 37°C, 5% $CO_2$ incubator. The growth medium was discarded the next day and replaced with 10 mL of pre-

warmed (37°C) complete DMEM. The cells were examined daily under an inverted microscope (Hund Wetzlar Wilovert S) to evaluate cell health and confluency. When cells displayed steady growth, the media was changed every two to three days, until the cells reached approximately 80% confluency. It was crucial to prevent cells from becoming and remaining overconfluent for more than two days since they may suffer from irreversible contact inhibition.

### *3.6.3. Cell Splitting*

When the cells reached approximately 80% confluency, cell splitting was executed. DMEM and 1x trypsin-EDTA were placed in a 37°C water bath for 10 minutes. Using a 10 mL serological pipette, DMEM was removed from the tissue culture flask. Then, 1 mL of trypsin-EDTA was added to the tissue culture flask which was gently mixed back and forth to ensure complete coverage of the cells with the solution. Cells were incubated at 37°C for 5 minutes, with frequent examination under a microscope to evaluate cell detachment. The flask was gently tapped against the bench surface to aid in cell detachment. Once the cells had detached, 9 mL of DMEM was added to the tissue culture flask in order to neutralize the trypsin-EDTA solution, the cells were collected. A split ratio of 1:5 was used, with some of the cells being frozen and the rest replated into 48 well plates for ultimate use with the samples in cell culture studies.

### *3.6.4. Cell Culturing on Sample Surfaces*

Previously prepared unmodified and APBA-modified pHEMA discs were placed inside the biosafety cabinet so that they may be exposed to UV light for 24 hours for sterilization and subsequently incubated in DMEM for 24 hours. Furthermore, in order to ensure that any cell adhesion that may occur will occur solely on the pHEMA surfaces rather than the well plate itself, the wells of a 48-well plate were blocked using a 2% alginate solution[85]. After exposure to UV light, eight unmodified and APBA-modified pHEMA discs were placed in the alginate wells

and incubated in 200 μL of DMEM for 24 hours. Following the previously described cell splitting procedure, surfaces were removed from the well plate and transferred into a new well plate. Then, 40 μL of cell suspension was carefully dispensed on each surface. Surfaces were then incubated for 30 minutes. This was to ensure that cells had sufficient time to bind to the surface rather than slide underneath the surfaces inside the well plate. Following incubation, 200 μL of fresh DMEM was dispensed into the well around the perimeter of the surface. The well plate was incubated, and media was replaced with 150 μL of fresh DMEM daily until cells reached 80% confluence.

#### *3.6.4.1. Cell Viability Assay*

In order to measure cell viability on the unmodified and APBA-modified pHEMA discs, an MTT assay was used. This is a photosensitive tetrazolium dye assay, in which yellow 3-(4,5-dimethylthiazol-2-yl)-2,5-diphenyltetrazolium bromide (MTT) is reduced to purple (*E,Z*)-5-(4,5-dimethylthiazol-2-yl)-1,3-diphenylformazan crystals (more commonly referred to as formazan) within living cells. Therefore, a deeper colour of formazan is an indicator of higher cell viability[86].

When cells reached 80% confluency, 20 μL of the MTT solution (0.5 mg/mL) was dispensed into each well, followed by a four-hour incubation period. Then, 100 μL of isopropanol was added to each well in order to solubilize the purple formazan crystals. Following complete solubilization, 100 μL of the solution from each well containing unmodified pHEMA and APBA-modified pHEMA discs was dispensed into empty wells for reading. The well plate was wrapped in tin foil to avoid light exposure when being transferred to the plate reader. The absorbance of the samples was measured using a Tecan M200 microplate reader at a wavelength of 580 nm with a reference wavelength of 680 nm.

# 4. Results and Discussion

## *4.1. Polymer Characterization*

### *4.1.1. Surface Chemical Composition*

#### *4.1.1.1. Attenuated Total Reflectance-Fourier Transform Infrared Spectroscopy (ATR-FTIR)*

The chemical composition of the materials' surface was first examined using ATR-FTIR spectroscopy. The spectra of all four steps of modification are shown in Figure 11a, and regions of interest are highlighted within Figure 11b/c.

There are three main peaks of interest within this spectrum. The first peak is highlighted in spectrum (b) and appears around 3150-3600 $cm^{-1}$ on the unmodified pHEMA surface and APBA-modified surfaces, but not the intermediate materials (pHEMA-Initiator and pHEMA-Methacrylate). According to literature, the alcohol (OH) stretch appears at approximately 3200-3600 $cm^{-1}$. The disappearance of this peak in the intermediate materials is indicative of the successful grafting of the initiator sites on the pHEMA surface. In the case of ATRP, this is the addition of the bromine initiator sites (~650 $cm^{-1}$)[87], and in the case CFRP, this is the addition of the vinyl group (~1650 $cm^{-1}$)[88]. However, the peak is reintroduced in the pHEMA-APBA materials due to the presence of alcohol in the boronic acid structure.

The second peak of interest can be seen in spectrum (c) around 1535 $cm^{-1}$. The amine (NH) group appears around 1580-1655 $cm^{-1}$, and can be seen in only the APBA-modified surfaces[89]. This essentially represents the acrylamide portion of the APBA structure, which serves as the tether for APBA attachment on the pHEMA surface. The absence of this peak from

the other materials further confirms the successful modification of the intermediate materials with APBA.

The final peak of interest can also be seen in spectrum (c) around 1350 $cm^{-1}$, and this represents the B-O stretch[90]. This peak is only present in the APBA-modified materials, confirming the successful grafting of APBA onto the pHEMA surface.

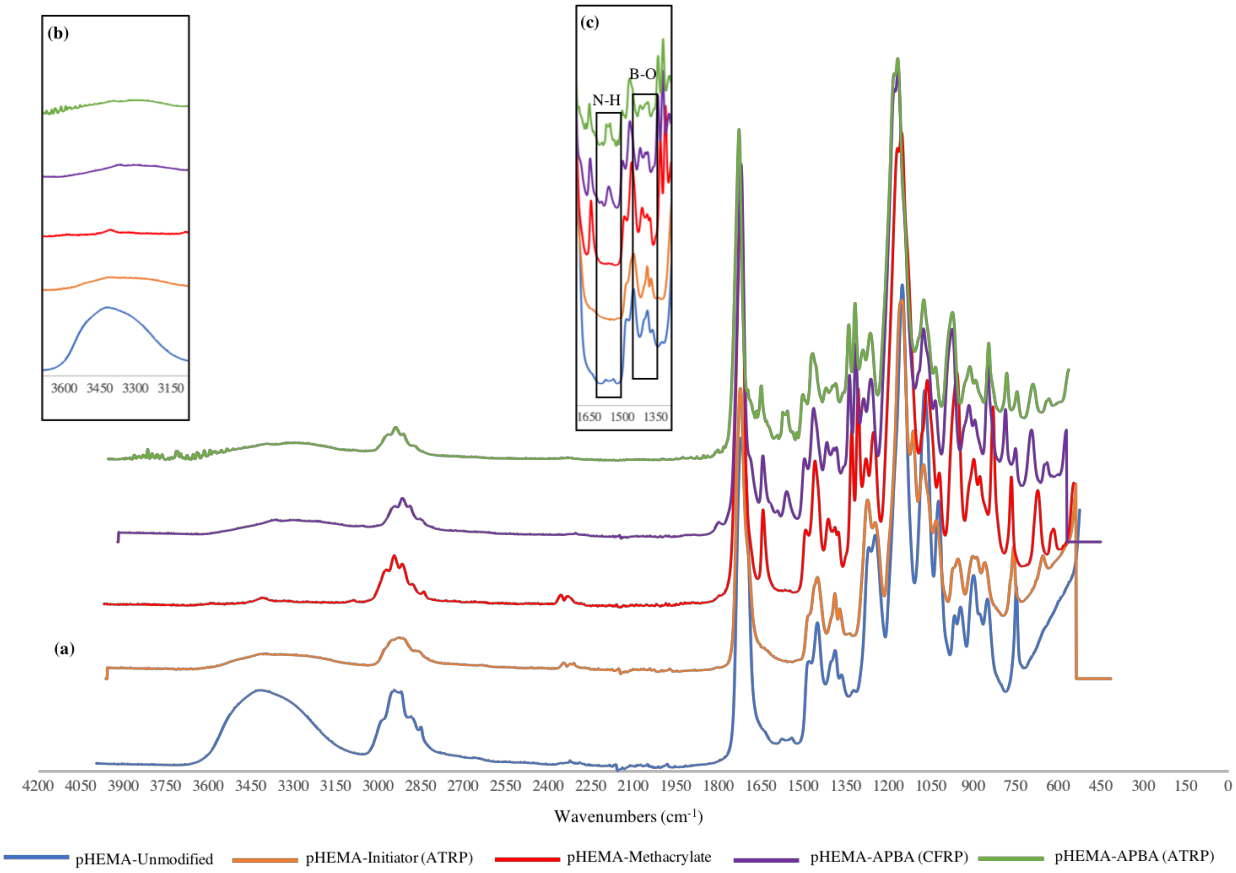


**Figure 11.** ATR-FTIR spectrum of all pHEMA surface modifications. **(a)** Full view of all surface modification steps. **(b)** Spectrum highlighting the O-H stretch around approximately 3150-3600 $cm^{-1}$. **(c)** Spectrum highlighting the N-H and B-O stretch around 1500 $cm^{-1}$ and 1350 $cm^{-1}$, respectively.

#### *4.1.1.2. X-ray Photoelectron Spectroscopy (XPS)*

Since FTIR-ATR spectroscopy only confirms the presence or absence of specific functional groups on the surface, quantification of the surface chemistry can be acquired through XPS (Table 1). This characterization technique was used to analyze the surface chemistry of

materials that were previously modified using the same protocols as discussed in this work.

The unmodified pHEMA material did not possess any boron content, as would be expected, and the C/O ratio is approximately in accordance with the theoretical composition of pHEMA based on its structure[91]. When observing the APBA-modified materials using CFRP and ATRP, one can note that boron is now present on the surface. Surfaces that were modified using ATRP possessed a greater percentage of boron than surfaces that were modified using CFRP. This is in accordance with the hypothesis that materials modified using ATRP will yield more phenylboronic acid on the surface due to the highly controlled nature of the polymerization method. Surfaces that were created using CFRP likely yielded a surface that possessed polymer chains that were of uneven lengths with an uneven distribution across the surface, likely resulting in a lower percentage of boron compared to surfaces created using ATRP.

The reaction mechanism of ATRP is reliant on the reversible transfer of the halogen atom from a polymeric surface to a transition metal complex in its lower oxidation state. This forms an active radical and the transition metal complex which is now in its higher oxidation state, and the transferred halogen atom is donated to the growing radical, in order to suppress (but not completely eliminate) growth, forming a dormant species. Therefore, the use of a transition metal is important for the success of ATRP. XPS did not detect the presence of copper in the sample. Following ATRP, surfaces exhibited a dark green colour and this is indicative of the copper catalyst that was used as part of the reaction. This green colour was observed even after surfaces were extracted using the Soxhlet method (3.4.3).

**Table 1.** Elemental composition (atom %) obtained with XPS at takeoff angle 45° recorded for previously unmodified and modified materials using the same protocol as discussed in this work.

| | **Takeoff angle of 45° Elemental Composition (as atom %)** | | | | | | | | | |
|---|---|---|---|---|---|---|---|---|---|---|
| | **C (1s)** | **O (1s)** | **B (1s)** | **N (1s)** | **Si (2p)** | **S (2p)** | **Ca (2p)** | **F (1s)** | **Pb (4f)** | **Cl (2p)** |
| **pHEMA-Unmodified** | 68.77 | 20.76 | - | - | 9.21 | 1.29 | 0.82 | - | - | - |
| **pHEMA-APBA (CFRP)** | 68.82 | 24.71 | **1.83** | 3.77 | 0.39 | - | - | 0.25 | 0.06 | 0.16 |
| **pHEMA (ATRP)** | 66.69 | 21.31 | **1.98** | 1.85 | 7.6 | - | - | - | - | - |

#### *4.1.1.3. Surface Wettability*

The wettability of the surfaces was measured using the sessile drop technique. This measures the contact angle between a solid surface (disc) and the liquid phase (water). A lower contact angle (< 90°) indicates a more wettable (hydrophilic) surface, whereas a greater contact angle (> 90°) indicates a less wettable (hydrophobic) surface. The contact angle measurements of the unmodified and APBA-modified materials are shown in Figure 12. This measurement served as further confirmation that surface composition was changed following modification. Due to the hydrophobic nature of APBA, it was hypothesized that contact angle should increase following modification. Furthermore, this hydrophobicity should be more pronounced on the surfaces modified using ATRP, due to the more uniform monolayer of APBA on the surface.

The unmodified material revealed a contact angle of approximately 75°, which is within the range of values that is found in the literature, using the sessile drop method[92–94]. Upon modification of the pHEMA surface with APBA, the contact angle showed a slight but insignificant increase. This can be attributed to the hydrophobic nature of APBA which has now

replaced the hydrophilic hydroxyl groups on the unmodified pHEMA surface. This hydrophobicity comes from the aromatic ring present in the APBA structure[95].

Surfaces that were modified using ATRP showed a significant increase in hydrophobicity, relative to unmodified surfaces ($p < 0.05$). This increase in hydrophobicity may be explained by the dense APBA chains that have been formed on the surfaces, as opposed to the chains formed using CFRP. In the case of the latter technique, there is no control over polymer chain length or the grafting density, and so it is possible that the water droplet may have been placed on an area on the disc that may have been populated by shorter chains. However, the difference in contact angle between the two modified surfaces is not significant. This may be indicative of comparable surface densities on both modified surfaces despite the different polymerization techniques used.

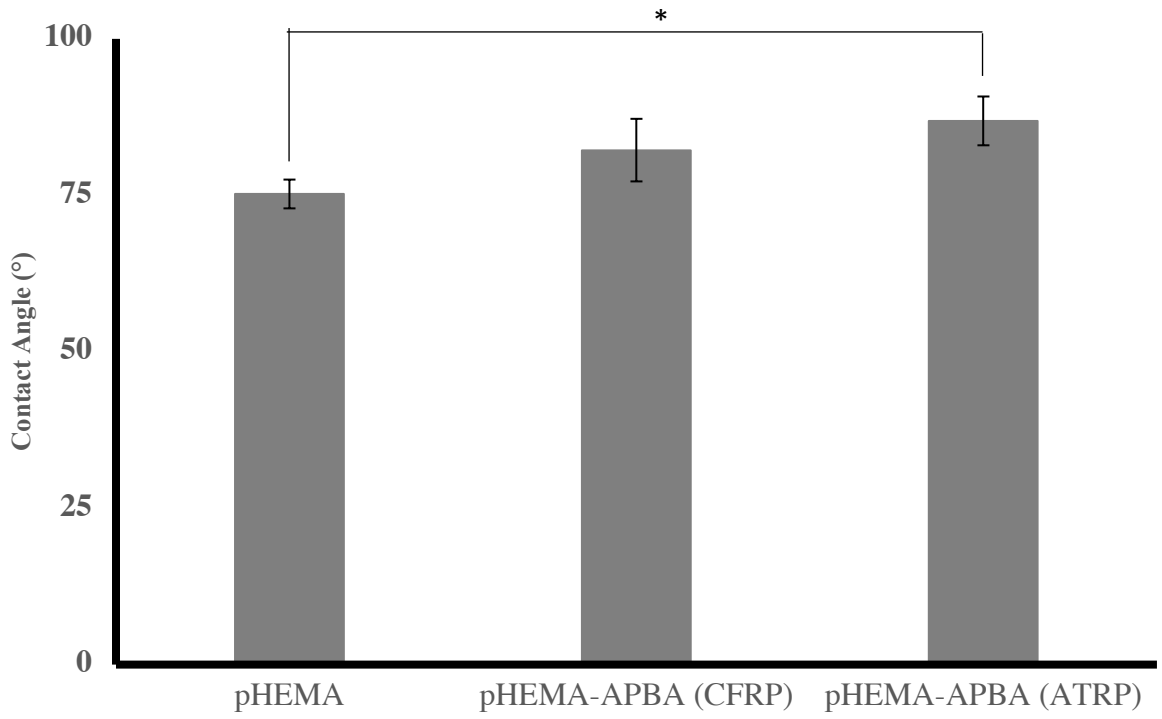


**Figure 12**. Water contact angle measurements for all materials. Data shown represents mean ± SD (n=4)

### *4.2. Cell Viability*

The viability of the cells seeded on the surfaces was evaluated using an MTT assay. This is a colourimetric assay that involves the reduction of the yellow MTT agent into purple formazan by viable cells. A greater concentration of viable cells will be indicated by a deeper purple solution in the wells and a high absorbance reading. The viability of the cells seeded on all surfaces, including a control well with no scaffold, can be seen in Figure 13.

The assay revealed little cell viability on the unmodified pHEMA surface and no cell viability on both modified surfaces. This was evident through the lack of colour change in the wells, as well as the absorbance values that were negligible in comparison to wells which did not contain any surfaces. It was expected that the unmodified pHEMA surfaces would not induce significant cell adhesion as these surfaces are inherently cell-repellent[19,96]. The lack of cell viability on both of the APBA-modified surfaces may be explained by the increase in hydrophobicity, surface density of APBA, and the presence of copper on the surfaces modified through ATRP.

The mechanism of cell adhesion to the extracellular matrix (ECM) and material surfaces is not fully understood, but it is known that adhesion is mediated by receptor proteins found in the cell membrane[97]. The group of receptor proteins that are responsible for cell adhesion to foreign substrates are known as integrins, and the proteins that have been of particular importance for cell adhesion to surfaces are fibronectin, laminin and vitronectin. Within each of these proteins is a particular peptide sequence that mediates cellular interactions with surfaces, such as arginine-glycine-aspartic acid (RGD) sequence in fibronectin and the tyrosine-isoleucine-glycine-serine-arginine (YIGSR) sequence in laminin. The presence of these proteins and their respective sequences has been shown to aid in cell adhesion to substrates[14,98–100]. However, hydrophobic

surfaces have the ability to induce non-specific protein adsorption[101,102]. The formation of this monolayer of proteins not only blocks cellular adhesion, but may also have long-term adverse effects. The contact angles (4.1.1.3) observed on all surfaces indicated more hydrophobic properties, and may have resulted in this non-specific protein adsorption. Additionally, the culture media used contained fetal bovine serum (FBS). This serum contains albumin, which can inhibit cell adhesion and also lacks the fibrinogen clotting agents. The presence of albumin and the absence of fibrinogen may have contributed to the lack of cell attachment on the surface.

The lack of cell viability on the modified surfaces may also be influenced by the grafting density of the APBA chains on the surface. The two polymerization techniques create surfaces that have different APBA chain densities. The CFRP technique creates chains that are unevenly distributed across the surface. This can result in cells failing to interact sufficiently with APBA units on the surface. However, ATRP allows for a much more controllable polymerization process, and so APBA chains formed through this technique are of equal length and with a more uniform distribution, resulting in a higher density. However, there are two factors that may be contributing to the lack of cell growth seen on these surfaces. First, the chains produced through this polymerization technique may not have been significantly longer than those created through the CFRP technique, as suggested by the insignificant difference in contact angle between the two surfaces. Therefore, cells may not have been able to interact with the APBA units on this surface. Second, the lack of cell viability may also be due to the presence of copper on the surface. This metal is intermixed within the material and either blocks cell adhesion or exerts toxic effects on the cells once they have adhered.

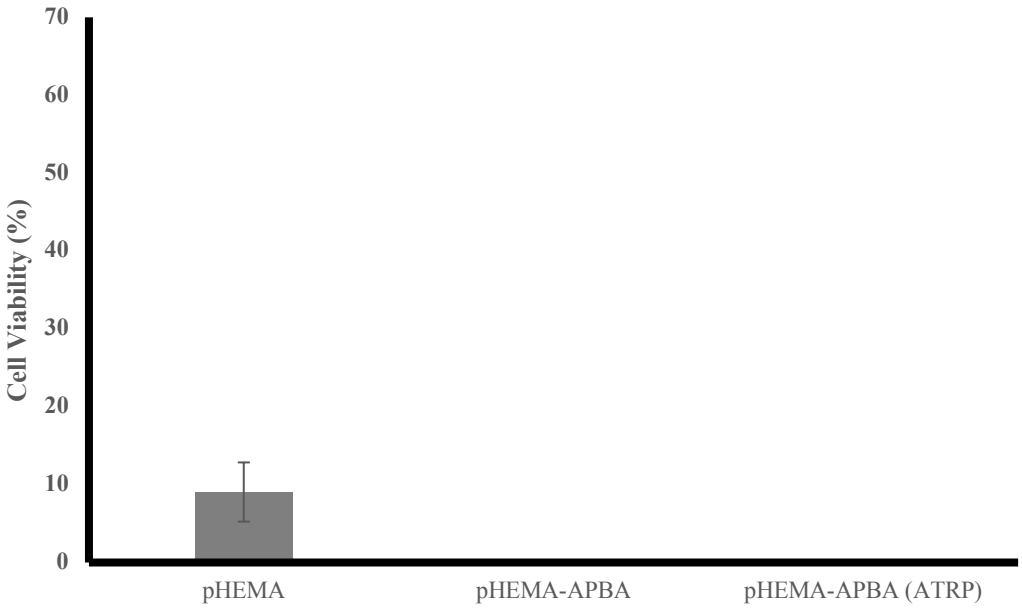


**Figure 13.** Cell viability (%) on all surfaces (n=8).

## 5. Conclusions

The pHEMA surface was successfully modified with APBA using CFRP and ATRP techniques, likely yielding polymer brushes of different architectures and surface densities, although this has not yet been confirmed by further testing. This modification was characterized through FTIR-ATR spectroscopy, XPS and surface wettability through contact angle measurements using the sessile drop technique. All of these characterization techniques indicated the successful grafting of APBA on the pHEMA surface. However, the modified surfaces did not perform well in cell culture as cell viability measured through an MTT assay indicated 0% viability. The factors influencing this lack of cell viability may be attributed to the hydrophobicity of the surface induced by the addition of APBA. This can result in non-specific protein adsorption which blocks cell adhesion. Specifically, the presence of albumin and absence of fibrinogen in the serum present in the culture media may have contributed to the lack of cell adhesion on the surfaces.

The surface density of APBA chains on the surfaces may also be a contributing factor to the lack of cell viability. The CFRP technique likely produces a surface with a non-uniform surface density of APBA chains that also vary in length. Therefore, the interaction of the cells with the surface may have been with an area that had low APBA chain density or with chains that were of an insufficient length to induce cellular interactions. It may be that the distribution of APBA chains formed through ATRP are more uniform, but these surfaces did not demonstrate cell-adhering capabilities potentially due to the toxicity that has been induced by the reaction mechanism. This technique relies on the use of a transition metal catalyst and this becomes intermixed into the material and can be toxic to the cells. It is necessary to investigate the polymer chain architecture on the modified surfaces as well as quantify the copper content within

the ATRP surfaces in order to gain an understanding as to which of these factors is contributing to the lack of cell viability.

Overall, it is possible that the modification of a polymer surface with PBA alone may not be sufficient to create a surface that has the potential to promote epithelialization. Future experimentation should evaluate the molecular weights and the distributions of the polymer chains constructed on these surfaces, as well as explore the effects that different concentrations, grafting densities, and chain lengths can have on surface wettability, cell viability and protein adsorption. Also, it is beneficial to explore the addition of cell adhesion proteins or peptide sequences in combination with PBA to aid cell attachment. Additionally, non-specific protein adsorption may be limited through the addition of substances that repel proteins from the surface of the material and allow for cellular interactions with polymer brush monolayer. Once cell adhesion has been established on the surface, it is necessary to evaluate the potential of cells to proliferate and migrate to cover the entire material's surface.

## 6. References


1. DelMonte, D. & Kim, T. Anatomy and physiology of the cornea and related structures. *J Cataract Refract Surg* **37,** 588–598 (2011).
2. Zieske, J. Perpetuation of stem cells in the eye. *Eye* **8,** 163–169 (1994).
3. Cortina, M. & de la Cruz, J. *Keratoprostheses and Artificial Corneas: Fundamentals and Surgical Applications*. (Springer, 2015).
4. Wright, B., Mi, S. & Connon, C. Towards the use of hydrogels in the treatment of limbal stem cell deficiency. *Drug Discov. Today* **18,** 79–86 (2013).
5. Klufas, M. & Colby, K. The Boston Keratoprosthesis. *Int. Ophthalmol. Clin.* **50,** 161–175 (2010).
6. Hicks, C. R. *et al.* Development and clinical assessment of an artifical cornea. *Prog. Retin. Eye Res.* **19,** 149–170 (2000).
7. Carlsson, D., Li, F., Shimmura, S. & Griffith, M. Bioengineered corneas: How close are we? *Curr. Opin. Ophthalmol.* **14,** 192–197 (2003).
8. Khan, B., Dudenhoefer, E. & Dohlman, C. Keratoprosthesis : an update. *Curr. Opin. Ophthalmol.* **12,** 282–287 (2001).
9. Shortt, A., Tuft, S. & Daniels, J. Corneal stem cells in the eye clinic. *Br. Med. Bull.* **100,** 209–225 (2011).
10. Chirila, T. *et al.* Artificial cornea. *Prog. Polym. Sci.* **23,** 447–473 (1998).
11. Griffith, M. *et al.* Artificial human corneas. *Cornea* **21,** 54–61 (2002).
12. Howard, D., Buttery, L., Shakesheff, K. & Roberts, S. Tissue engineering: Strategies, stem cells and scaffolds. *J. Anat.* **213,** 66–72 (2008).
13. Hicks, C., Chirila, T., Vijayasekaran, S. & Crawford, G. pHEMA as a keratoprosthesis material. *Br. J. Ophthalmol.* **90,** 123–124 (2005).
14. Merrett, K., Griffith, C., Deslandes, Y., Pleizier, G. & Sheardown, H. Adhesion of corneal epithelial cells to cell adhesion peptide modified pHEMA surfaces. *J. Biomater. Sci. Polym. Ed.* **12,** 647–671 (2001).
15. Klenkler, B., Griffith, M., Becerril, C., West-Mays, J. & Sheardown, H. EGF-grafted PDMS surfaces in artificial cornea applications. *Biomaterials* **26,** 7286–7296 (2005).
16. Klenkler, B., Dwivedi, D., West-Mays, J. & Sheardown, H. Corneal epithelial cell adhesion and growth on EGF-modified aminated PDMS. *J. Biomed. Mater. Res. - Part A* **93,** 1043–1049 (2010).
17. Cambre, J. & Sumerlin, B. Biomedical applications of boronic acid polymers. *Polymer (Guildf).* **52,** 4631–4643 (2011).
18. Brooks, W. & Sumerlin, B. Synthesis and Applications of Boronic Acid-Containing Polymers: From Materials to Medicine. *Chem. Rev.* **116,** 1375–1397 (2016).
19. Pan, G. *et al.* Dynamic introduction of cell adhesive factor via reversible multicovalent phenylboronic acid/ cis -diol polymeric complexes. *J. Am. Chem. Soc.* **136,** 6203–6206 (2014).
20. Zdyrko, B. & Luzinov, I. Polymer brushes by the 'grafting to' method. *Macromol. Rapid Commun.* **32,** 859–869 (2011).
21. Edmondson, S., Osborne, V. L. & Huck, W. T. S. Polymer Brushes via surface-initiated polymerization. 14–22 (2004).
22. Meek, K. M. & Knupp, C. Corneal structure and transparency. *Prog. Retin. Eye Res.* **49,** 1–16 (2015).

23. Dua, H., Gomes, J. & Singh, A. Corneal epithelial wound healing. *Br J Ophthalmol* **78,** 401–408 (1994).
24. Schermer, A., Galvin, S. & Sun, T. Differentiation-related expression of a major 64K corneal keratin in vivo and in culture suggests limbal location of corneal epithelial stem cells. *J. Cell Biol.* **103,** 49–62 (1986).
25. McCaa, C. The eye and visual nervous system: anatomy, physiology and toxicology. *Environ. Health Perspect.* **Vol. 44,** 1–8 (1982).
26. Farjo, A., McDermott, M. & Soong, H. Corneal anatomy, physiology and would healing. in *Ophthalmology* (eds. Yanoff, M. & Duker, J.) 203–208 (Mosby, 2008).
27. Cameron, J. *Corneal reaction to injury*. (2005).
28. Wiley, L., SundarRaj, N., Sun, T. & Thoft, R. Regional heterogeneity in human corneal and limbal epithelia: an immunohistochemical evaluation. *Invest Ophthalmol Vis Sci* **32,** 594–602. (1991).
29. Hersh, P., Zarbin, M., Fisher, E., Dua, H. & Azuara-Blanco, A. Limbal Stem Cells of the Corneal Epithelium. *Surv. Ophthalmol.* **44,** 415–425 (2000).
30. Daniels, J., Dart, J., Tuft, S. & Khaw, P. Corneal stem cells in review. *Wound repair Regen.* **9,** 483–494 (2001).
31. Akkaya, Z. Limbal epithelial stem cells. *Niche* **3,** 52–57 (2012).
32. Yeung, A. *et al.* Limbal epithelial crypt: a model for corneal epithelial maintenance and novel limbal regional variations. *Arch. Ophthalmol.* **126,** 665–669 (2008).
33. Dua, H., Gomes, J., King, A. & Maharajan, V. The amniotic membrane in ophthalmology. *Surv. Ophthalmol.* **49,** 51–77 (2004).
34. Bettman, J. Nature of Bowman's layer. *N. Engl. J. Med.* **282,** 344 (1970).
35. Tisdale, A. *et al.* Development of anchoring structres of the epithelium in rabbit and human fetal corneas. *Invest. Ophthalmol. Vis. Sci.* **26,** 59–68 (1988).
36. Komai, Y. & Ushiki, T. The three-dimensional organization of collagen fibrils in the human cornea and sclera. *Invest. Ophthalmol. Vis. Sci.* **32,** 2244–2258 (1991).
37. Mishima, S. Corneal Thickness. *Surv. Ophthalmol.* **13,** 57–96 (1968).
38. Schmoll, T. *et al.* Precise thickness measurements of Bowman's layer, epithelium, and tear film. **89,** 795–802 (2012).
39. Lagali, N., Germundsson, J. & Fagerholm, P. The role of Bowman's layer in corneal regeneration after phototherapeutic keratectomy: A prospective study using in vivo confocal microscopy. *Investig. Ophthalmol. Vis. Sci.* **50,** 4192–4198 (2009).
40. Wilson, S. & Hong, J. Bowman's layer structure and function: Critical or dispensable to corneal function? A Hypothesis. *Cornea* **19,** 417–420 (2000).
41. Chakravarti, S. *et al.* Lumican regulates collagen fibril assembly: Skin fragility and corneal opacity in the absence of lumican. *J. Cell Biol.* **141,** 1277–1286 (1998).
42. Corpuz, L. *et al.* Molecular cloning and tissue distribution of keratocan. *J. Biol. Chem.* **271,** 9759–9763 (1996).
43. Funderburgh, J. *et al.* Nucleic acids, protein synthesis, and molecular genetics: Mimecan, the 25-kDa corneal keratan sulfate proteoglycan is a product of the gene producing osteoglycin. **272,** 28089–28095 (1997).
44. Jester, J. *et al.* The cellular basis of corneal transparency: evidence for 'corneal crystallins'. *J. Cell Sci.* **112 ( Pt 5,** 613–622 (1999).
45. West-Mays, J. & Dwivedi, D. The keratocyte: Corneal stromal cell with variable repair phenotypes. *Int. J. Biochem. Cell Biol.* **38,** 1625–1631 (2006).

46. Levy, S., Moss, J., Sawada, H., Dopping-Hepenstal, P. & McCartney, A. The composition of wide-spaced collagen in normal and diseased Descemet's membrane. *Curr. Eye Res.* **15,** 45–52 (1996).
47. Stephan, S., Sherratt, M., Hodson, N., Shuttleworth, C. & Kielty, C. Expression and supramolecular assembly of recombinant α1(VIII) and α2(VIII) collagen homotrimers. *J. Biol. Chem.* **279,** 21469–21477 (2004).
48. Hopfer, U. Targeted disruption of Col8a1 and Col8a2 genes in mice leads to anterior segment abnormalities in the eye. *FASEB J.* **19,** 1232–1244 (2005).
49. Bourne, W., Nelson, L. & Hodge, D. Central corneal endothelial cell changes over a ten-year period. *Invest. Ophthalmol. Vis. Sci.* **38,** 779–782 (1997).
50. Hanna, C. & O'Brien, J. E. Cell Production and of the Cornea Migration in the Epithelial Layer. *Arch. Ophthalmol.* **64,** 536–539 (1960).
51. Hanna, C., Bicknell, D. & O'Brien, J. Cell Turnover in the Adult Human Eye. *Arch. Ophthalmol.* **65,** 695–698 (1961).
52. Khoudadoust, A., Silverstein, A., Kenyon, K. & Dowling, J. Adhesion of regenerating corneal epithelium: the role of basement membrane. *Am. J. Opthalmology* **65,** 339–348 (1968).
53. Hirst, L., Kenyon, K., Fogle, J., Hanninen, L. & Stark, W. Comparative Studies of Corneal Surface Injury in the Monkey and Rabbit. *Arch. Ophthalmol.* **99,** 1066–1073 (1981).
54. Tosi, G., Massaro-Giordano, M., Caporossi, A. & Toti, P. Amniotic membrane transplantation in ocular surface disorders. *J. Cell. Physiol.* **202,** 849–851 (2005).
55. Deshpande, P. *et al.* Deshpande et al 2009 Development_of_a_surface-modif.PDF. *Tissue Eng. Part A* **15,** 2889–2902 (2009).
56. Bobba, S. & Di Girolamo, N. Contact lenses: A delivery device for stem cells to treat corneal blindness. *Optom. Vis. Sci.* **93,** 412–418 (2016).
57. Aucoin, L., Griffith, C., Pleizier, G. & Deslandes, Y. Interactions of corneal epithelial cells and surfaces modi ed with cell adhesion peptide combinations. **13,** 447–462 (2002).
58. Duan, D., Klenkler, B. J. & Sheardown, H. Progress in the development of a corneal replacement: Keratoprostheses and tissue-engineered corneas. *Expert Rev. Med. Devices* **3,** 59–72 (2006).
59. Ayres, N. Polymer brushes: Applications in biomaterials and nanotechnology. *Polym. Chem.* **1,** 769–777 (2010).
60. Xu, F. J., Neoh, K. G. & Kang, E. T. Bioactive surfaces and biomaterials via atom transfer radical polymerization. *Prog. Polym. Sci.* **34,** 719–761 (2009).
61. Prucker, O. & Rühe, J. Polymer Layers through Self-Assembled Monolayers of Initiators. *Langmuir* **14,** 6893–6898 (1998).
62. Jones, R., Lehnert, R., Schönherr, H. & Vancso, J. Factors affecting the preparation of permanently end-grafted polystyrene layers. *Polymer (Guildf).* **40,** 525–530 (1999).
63. Zhao, B. & Brittain, W. Polymer brushes: Surface-immobilized macromolecules. *Prog. Polym. Sci.* **25,** 677–710 (2000).
64. Moad, G. & Solomon, D. *The Chemistry of Free Radical Polymerization*. (Pregamon, 1995).
65. Coessens, V., Pintauer, T. & Matyjaszewski, K. Functional polymers by atom transfer radical polymerization. *Prog. Polym. Sci.* **26,** 337–377 (2001).
66. Matyjaszewski, K. Atom Transfer Radical Polymerization (ATRP): Current status and

future perspectives. *Macromolecules* **45,** 4015–4039 (2012).
67. Kamigaito, M., Ando, T. & Sawamoto, M. *Metal-catalyzed living radical polymerization*. *Chemical Reviews* **101,** (2001).
68. Strohbach, A. & Busch, R. Polymers for Cardiovascular Stent Coatings. *Int. J. Polym. Sci.* **2015,** (2015).
69. Dailey, M. *et al.* A self-healing biomaterial based on free-radical polymerization. *J. Biomed. Mater. Res. - Part A* **102,** 3024–3032 (2014).
70. Xiong, Y., Li, M., Lu, Q., Qing, G. & Sun, T. Sialic acid-targeted biointerface materials and bio-applications. *Polymers (Basel)*. **9,** (2017).
71. Lorand, J. & Edwards, J. Polyol complexes and structure of the benzeneborate ion. *J. Org. Chem.* **24,** 769–774 (1959).
72. Wulff, G. Selective binding to polymers via covaent bonds: The construction of chiral cavities as specific receptor sites. *Construction* **54,** 2093–2102 (1982).
73. Kikuchi, A. *et al.* Glucose-sensing electrode coated with polymer complex gel containing phenylboronic acid. *Anal. Chem.* **68,** 823–828 (1996).
74. Matsumoto, A., Sato, N., Kataoka, K. & Miyahara, Y. Noninvasive sialic acid detection at cell membrane by using phenylboronic acid modified self-assembled monolayer gold electrode. *J. Am. Chem. Soc.* **131,** 12022–12023 (2009).
75. Wang, X., Xia, N. & Liu, L. Boronic acid-based approach for separation and immobilization of glycoproteins and its application in sensing. *Int. J. Mol. Sci.* **14,** 20890–20912 (2013).
76. Egawa, Y., Miki, R. & Seki, T. Colorimetric sugar sensing using boronic acid-substituted azobenzenes. *Materials (Basel)*. **7,** 1201–1220 (2014).
77. Lorand, J. P. & Edwards, J. O. Polyol Complexes and Structure of the Benzeneboronate Ion. *J. Org. Chem.* **24,** 769–774 (1959).
78. Liu, H. *et al.* Dual-Responsive Surfaces Modified with Phenylboronic Acid-Containing Polymer Brush to Reversibly Capture and Release Cancer Cells Dual-Responsive Surfaces Modified with Phenylboronic Acid-Containing Polymer Brush to Reversibly Capture and Release Cancer C. (2013). doi:10.1021/ja401000m
79. Saito, A., Konno, T., Ikake, H., Kurita, K. & Ishihara, K. Control of cell function on a phospholipid polymer having phenylboronic acid moiety. *Biomed. Mater.* **5,** (2010).
80. Varki, A. Sialic acids in human health and disease. *Trends Mol Med.* **14,** 351–360 (2009).
81. Otsuka, H., Uchimura, E., Koshino, H., Okano, T. & Kataoka, K. Anomalous binding profile of phenylboronic acid with N-acetylneuraminic acid (Neu5Ac) in aqueous solution with varying pH. *J. Am. Chem. Soc.* **125,** 3493–3502 (2003).
82. Hirschberg, C., Goodman, S. & Green, C. Sialic Acid Uptake by Fibroblasts. *Biochemistry* **15,** 3591–3599 (1976).
83. Keller, R. & Wycoff, H. Purification of CuBr. *Inorg. Synth.* **2,** 1–4 (1946).
84. Karlgard, C., Sarkar, D., Jones, L., Moresoli, C. & Leung, K. Drying methods for XPS analysis of PureVision™, Focus® Night&Day™ and conventional hydrogel contact lenses. *Appl. Surf. Sci.* **230,** 106–114 (2004).
85. Wu, Z. *et al.* Bioprinting three-dimensional cell-laden tissue constructs with controllable degradation. *Sci. Rep.* **6,** 1–10 (2016).
86. Berridge, M. & Tan, A. Berridge et al 1993 Characterization of the cellular reduction of MTT. *Arch. Biochem. Biophys.* **303,** 474–482 (1993).
87. Urbaniak-domagala, W. The Use of the Spectrometric Technique FTIR-ATR to Examine

the Polymers Surface. *Adv. Apects Spectrosc.* 86–104 (2012). doi:10.5772/2757
88. Nakamoto, K. *Infrared and Raman Spectra of Inorganic and Coordination Compounds*. (John Wiley & Sons., 2009).
89. Davaran, S., Hanaee, J. & Khosravi, A. Release of 5-amino salicylic acid from acrylic type polymeric prodrugs designed for colon-specific drug delivery. *J. Control. Release* **58,** 279–287 (1999).
90. Faniran, J. A. & Shurvell, H. F. Infrared spectra of phenylboronic acid (normal and deuterated) and diphenyl phenylboronate. *Can. J. Chem.* **46,** 2089–2095 (1968).
91. Castner, D. G., Ratner, B. D., Hirao, A. & Nakahama, S. Characterization of Poly(2-Hydroxyethyl Methacrylate) (PHEMA) by XPS. *Surf. Sci. Spectra* **4,** 14–20 (1996).
92. Holly, J. & Refojo, J. Wettability of Hydrogels Poly(2-Hydroxyethyl Methacrylate ). *J. Biomed. Mater. Res.* **9,** 315–326 (1975).
93. Morra, M., Occhiello, E. & Garbassi, F. On the wettability of poly(2-hydroxyethylmethacrylate). *J. Colloid Interface Sci.* **149,** 84–91 (1992).
94. Lim, H., Lee, Y., Han, S., Cho, J. & Kim, K. Surface treatment and characterization of PMMA, PHEMA, and PHPMA. *J. Vac. Sci. Technol. A Vacuum, Surfaces, Film.* **19,** 1490–1496 (2001).
95. Taleb, S., Noyer, E., Godeau, G., Darmanin, T. & Guittard, F. Switchable Surface Wettability by Using Boronic Ester Chemistry. *ChemPhysChem* **17,** 305–309 (2016).
96. Bhat, R. R., Chaney, B. N., Rowley, J., Liebmann-Vinson, A. & Genzer, J. Tailoring cell adhesion using surface-grafted polymer gradient assemblies. *Adv. Mater.* **17,** 2802–2807 (2005).
97. Horbett, T. A. The role of adsorbed proteins in animal cell adhesion. *Colloids Surfaces B Biointerfaces* **2,** 225–240 (1994).
98. Xie, R. Z. *et al.* Effects of biologically modified surfaces of synthetic lenticules on corneal epithelialization in vivo. *Aust. N. Z. J. Ophthalmol.* **25 Suppl 1,** S46-9 (1997).
99. Fittkau, M. H. *et al.* The selective modulation of endothelial cell mobility on RGD peptide containing surfaces by YIGSR peptides. *Biomaterials* **26,** 167–174 (2005).
100. Chang, H. & Wang, Y. *Cell Responses to Surface and Archecture of Tissue Engineering Scaffolds*. *Regenerative Medicine and Tissue Engineering - Cells and Biomaterials* (InTech, 2011).
101. Tamada, Y. & Yoshito, I. Effect of preadsorbed proteins on cell adhesion to polymer surfaces. *J. Colloid Interface Sci.* **155,** 334–339 (1993).
102. Malmsten, M., Emoto, K. & Alstine, J. M. Van. Effect of Chain Density on Inhibition of Protein Adsorption by Poly (ethylene glycol) Based Coatings. **517,** 507–517 (1998).

# 7. Appendix A: Experimental Procedures

## A.1: Cell Freezing

Following cell splitting, several cryovials were prepared each containing 50 µL of cell suspension with 1 mL of DMEM and 10% DMSO. The cryovials were then transferred into liquid nitrogen for storage until use.